OPTIMAL TRIANGULATION OF POLYGONS

CHRISTOPHER J. BISHOP

Abstract. How do we cut a polygon into triangles that are all as "round" as possible, e.g., minimizing the maximum angle used? In this paper, we give the optimal upper and lower angle bounds for triangulating a polygon P with Steiner points, and prove that triangulations attaining these bounds always exist, except in a few clearly defined cases. These results sharpen the 1960 theorem of Burago and Zalgaller that every n-gon has an acute triangulation. We show that the optimal bounds can be computed in time $O(n)$, even though there is no polynomial bound for size of the corresponding optimal triangulations. We also deduce that the optimal angle bounds for polygonal triangulations are the same as for triangular dissections. This implies, in a stronger form, a 1984 conjecture of Gerver.

Date: February 21, 2021; revised May 2, 2023.

1991 *Mathematics Subject Classification.* Primary: 30C62, Secondary: 68U05, 52C20 .

Key words and phrases. acute triangulation, Steiner points, dissections, Schwarz-Christoffel formula, Delaunay triangulation, Gerver's conjecture.

The author is partially supported by NSF Grant DMS 1906259.

1. Statement of results

It is a problem of long-standing theoretical and practical interest to triangulate a polygon with the best possible bounds on the angles used. For example, the constrained Delaunay triangulation famously maximizes the minimal angle if no additional vertices (called Steiner points) are allowed [42], [43], and algorithms for minimizing the maximum angle (again without Steiner points) are given in [7] and [28]. In this paper, we will compute the optimal upper and lower angle bounds for triangulating any polygon P when the finite collection of non-Steiner triangulations is replaced by the infinite dimensional family of triangulations allowing Steiner points.

In this case, Burago and Zalgaller [19] proved in 1960 that every planar polygon P has an acute triangulation (all angles $< 90°$). This is best possible if we want a uniform angle bound independent of P, and there is now a large collection of theorems, heuristics and software involving acute triangulations. However, several fundamental questions have remained open. What are the optimal upper and lower angle bounds for triangulating a given polygon P with Steiner points? Are these bounds attained or can they only be approximated? Can both bounds be attained simultaneously? How regular are the corresponding triangulations? How do the angle bounds for triangulations differ from those for dissections? Using ideas involving conformal and quasiconformal mappings, we shall answer each of these questions.

We start with some notation. Suppose $\mathcal{T}$ is a triangulation of P. Let V_P and $V_{\mathcal{T}}$ denote the vertex sets of P and $\mathcal{T}$ respectively and note $V_P \subset V_{\mathcal{T}}$. We define $\partial\mathcal{T} = V_{\mathcal{T}} \cap P$ to be the boundary vertices of $\mathcal{T}$, and let $\text{int}(\mathcal{T}) = V_{\mathcal{T}} \setminus \partial\mathcal{T}$ denote the interior vertices. Label each $v \in V_{\mathcal{T}}$ with the number, $L(v)$, of triangles in $\mathcal{T}$ that have v as a vertex. For $v \in \partial\mathcal{T}$, we define its discrete curvature as $\kappa(v) = 3 - L(v)$, and for an interior vertex we set $\kappa(v) = 6 - L(v)$. This notion of curvature for triangulations is implicit in Gerver's paper [33], explicit in Thurston's work [57], and has, no doubt, occurred elsewhere. See Figure 1. Using these definitions, Euler's formula applied to a triangulation can be rewritten to look like the Gauss-Bonnet formula:

$$\sum_{v \in \text{int}(\mathcal{T})} \kappa(v) = 6 - \sum_{v \in \partial\mathcal{T}} \kappa(v). \tag{1.1}$$

The common value is denoted $\kappa(\mathcal{T})$, the curvature of the triangulation.

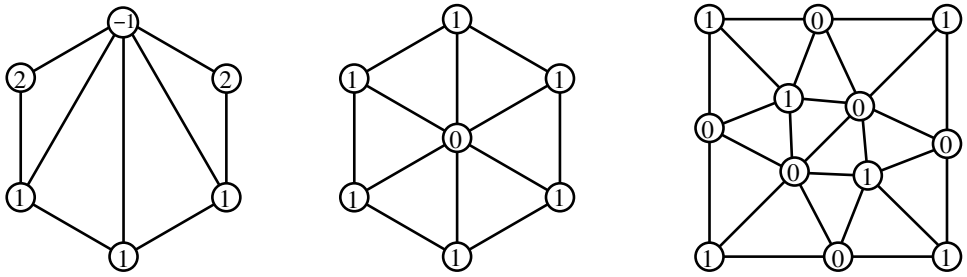

FIGURE 1. Vertices are labeled with their discrete curvatures; the triangulations have curvatures 0, 0, 2 respectively. The left and center show that allowing Steiner points can lower the maximum angle (here, from 120° to 60°). The center and right triangulations have the optimal upper angle bounds for a hexagon (60°) and a square (72°).

For $\phi > 0$, a ϕ-triangulation of P is one with all angles at most ϕ. For $\phi \in [60°, 90°]$ define the interval $I(\phi) = [180 - 2\phi, \phi]$. Since the angles of a triangle sum to 180°, it is easy to check that any ϕ-triangulation must have all of its angles in $I(\phi)$. Let $|V_P|$ be the number of vertices in P, and for $v \in V_P$, let θ_v denote the interior angle of P at v. A labeling $L : V_P \to \mathbb{N} = \{1, 2, \dots\}$ is called ϕ-admissible (or a ϕ-labeling) if $\theta_v \in L(v) \cdot I(\phi)$ for every $v \in V_P$. Note that this implies $L(v)(180° - 2\phi) \le \theta_v \le 360°$, so that elements of a ϕ-admissible labeling all lie between 1 and $\lfloor 360/(180 - 2\phi) \rfloor$. The curvature of a labeling L is defined as

$$\kappa(L) = 6 - \sum_{v \in V_P} \kappa(v) = 6 - \sum_{v \in V_P} (3 - L(v)) = 6 - 3|V_p| + \sum_{v \in V_P} L(v).$$

If a labeling L of V_P comes from a ϕ-triangulation $\mathcal{T}$ of P with $\phi < 90°$, then it is automatically ϕ-admissible and satisfies $\kappa(L) \le \kappa(\mathcal{T})$, since vertices of $\partial\mathcal{T} \setminus V_P$ must have degree ≥ 3 (see Section 9 for more details). If $\phi < 72°$ then $\text{int}(\mathcal{T})$ has no vertices of degree ≤ 5, so (1.1) implies $\kappa(L) \le \kappa(\mathcal{T}) \le 0$. See Figure 2. Similarly, if $\phi < \frac{5}{7} \cdot 90° \approx 64.2857°$ then every vertex in $\text{int}(\mathcal{T})$ has degree 6 and every vertex in $\partial\mathcal{T} \setminus V_P$ has degree 3, so $\kappa(L) = \kappa(\mathcal{T}) = 0$. Remarkably, these elementary necessary conditions are also sufficient.

Theorem 1.1. *For $60° < \phi \le 90°$, a polygon P has a ϕ-triangulation if and only if*

1. *$72° \le \phi < 90°$ and there is some ϕ-admissible labeling L of V_P,*
2. *$\frac{5}{7} \cdot 90° \le \phi < 72°$, and there is a ϕ-admissible labeling with $\kappa(L) \le 0$,*
3. *$60° < \phi < \frac{5}{7} \cdot 90°$, and there is a ϕ-admissible labeling with $\kappa(L) = 0$.*

For $60^\circ < \phi < 90^\circ$ define $\mathcal{K}(\phi)$ to be the set of possible values of $\kappa(L)$ over all ϕ-admissible labelings of V_P; we set $\mathcal{K}(\phi) = \infty$ if there is no admissible labeling. We claim that $\mathcal{K}(\phi)$ is either ∞ or a non-empty interval of integers. To see this, note that for each vertex v, the set of ϕ-admissible labels for v is $\{L \in \mathbb{N} : \theta_v/(180-2\phi) \leq L \leq \theta_v/\phi\}$. Thus the set of possible curvatures is either empty or a sum of integers, each taken from an interval, hence it is an interval itself.

Thus $\mathcal{K}(\phi)$ has a unique closest element to 0, denoted $\kappa(\phi)$ (possibly equal to 0 or ∞). The three conditions in Theorem 1.1 can be restated as $\kappa(\phi) < \infty$, $\kappa(\phi) \leq 0$ and $\kappa(\phi) = 0$ respectively. (We should write $\mathcal{K}(\phi, P)$ and $\kappa(\phi, P)$, since these quantities also depend on P, but in this paper P is usually fixed and clear from context.)

For a simple polygon P, define

$$\Phi(P) = \inf\{\phi : P \text{ has a } \phi\text{-triangulation }\}.$$

Is this infimum attained? Since the elements of a ϕ-admissible labeling are uniformly bounded, if P has a sequence of ϕ_n-labelings for $\phi_n \searrow \phi < 90^\circ$, then the same labeling occurs infinitely often, and must be a ϕ-labeling for P. Thus the non-strict inequalities in Cases 1 and 2 of Theorem 1.1 imply the following.

Corollary 1.2. *If $\Phi(P) > 60^\circ$, then $\Phi(P)$ is attained by some finite triangulation.*

On the other hand, if $\Phi(P) = 60^\circ$ then sometimes the infimum is attained and sometimes it is not. It is easy to verify that $\Phi(P) = 60^\circ$ implies every interior angle of P is an integer multiple of 60°; if this holds, we call P a 60°-polygon. Conversely, every 60°-polygon has $\Phi(P) = 60^\circ$; see Lemma 5.1. In a 60°-triangulation every triangle is equilateral and thus must have the same size, so such a triangulation exists for P if and only if any two edges of P have rational length ratio. Thus 60°-polygons that have some irrational edge length ratio are the only polygons for which the optimal bound $\Phi(P)$ is not attained by any triangulation of P. See Figure 2.

As noted earlier, Burago and Zalgaller [19] proved that $\Phi(P) < 90^\circ$ for any polygon P. Theorem 1.1 implies a sharp, explicit improvement of this.

Corollary 1.3. *For any polygon with minimal angle θ, $\Phi(P) \leq 90^\circ - \min(\theta, 36^\circ)/2$.*

This will be proven in Section 10. If a polygon P has an interior angle θ, then any triangulation of P contains a triangle T with some angle $\leq \theta$. Since the angles of

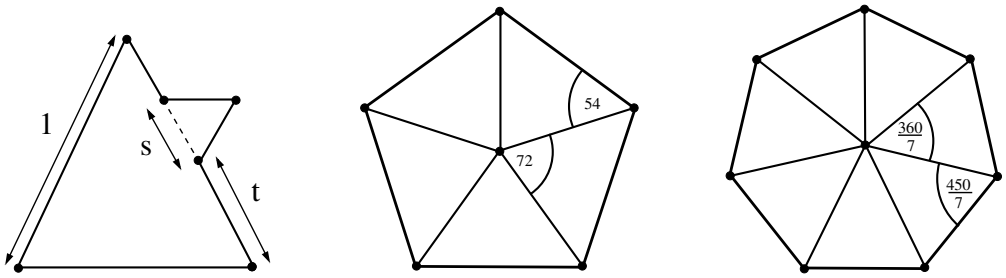

FIGURE 2. The left polygon satisfies $\kappa(60^\circ) = 0$, but has no equilateral triangulation unless both s and t are rational. The other pictures show where the special angles in Theorem 1.1 come from: these angles are forced by interior vertices of degree five or seven.

T sum to 180°, it also contains an angle $\geq 90^\circ - \theta/2$. Thus by Corollary 1.3, if the minimal angle is $\theta \leq 36^\circ$, then $\Phi(P) = 90^\circ - \theta/2$ and the optimal triangulation has all of its angles in $[\theta, 90^\circ - \theta/2]$. Also, $\Phi(P) \leq 72^\circ$ if its minimal angle is $\theta \geq 36^\circ$, strengthening a result of Gerver for dissections (Theorem 2, [33]). A triangular dissection of P is a finite collection of closed triangles that cover exactly P and its interior, and that have pairwise disjoint interiors. The edges of adjacent triangles in a dissection need not match up exactly; if they do, then we have a triangulation. See Figure 3. A ϕ-dissection is a triangular dissection with maximum angle $\leq \phi$. In 1984, Gerver [33] showed that the conditions in Theorem 1.1 are necessary if P has a $(\phi + \epsilon)$-dissection for every $\epsilon > 0$, and he conjectured that they are sufficient for a ϕ-dissection to exist if $\phi > 60^\circ$. Theorem 1.1 strengthens this by proving that these conditions actually imply a ϕ-triangulation exists.

Corollary 1.4. *For a polygon P and $\phi \in (60^\circ, 90^\circ]$, the following are equivalent:*

(1) *For every $\epsilon > 0$, P has a $(\phi + \epsilon)$-dissection,*
(2) *P has a ϕ-dissection,*
(3) *P has a ϕ-triangulation.*

This will be proven in Section 11; only (1) $\Rightarrow$ (3) needs to be verified, since (3) $\Rightarrow$ (2) $\Rightarrow$ (1) is trivial. The corollary implies that for every polygon P, we have $\Phi(P) = \mathcal{M}(P) \coloneqq \inf\{\phi : P \text{ has a } \phi\text{-dissection}\}$, using the notation from [33]. This is surprising (at least to the author). Since dissections satisfy much less stringent conditions than triangulations do, one might expect a gap $\Phi(P) > \mathcal{M}(P)$ for some polygons P, but such a gap never occurs. Corollary 1.2 implies that the infimum

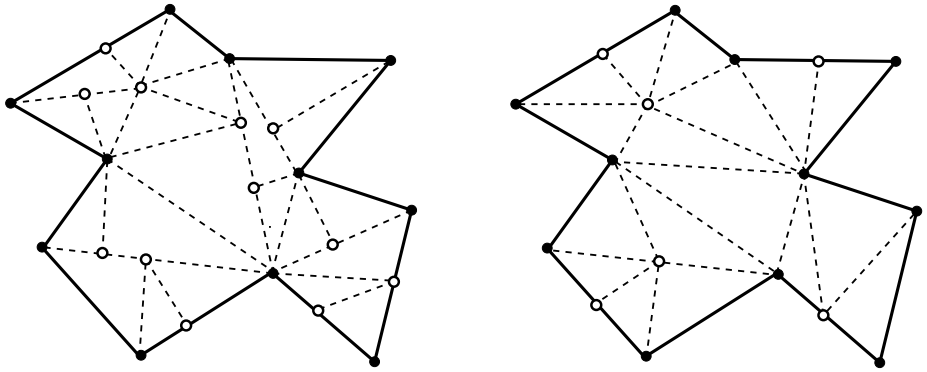

FIGURE 3. On the left is a dissection of a polygon and on the right a triangulation. The white dots are the Steiner points. Despite triangulations being more restrictive than dissections, the optimal upper angle bounds are the same for both types of decomposition.

defining $\mathcal{M}(P)$ is attained (by a triangulation) whenever $\mathcal{M}(P) > 60°$. However, Tutte [60] proved that a convex 60°-polygon does not have a dissection into equilateral triangles unless all of its side length ratios are rational (see also Theorem 4 of [39]). Thus an optimal dissection need not always exist when $\mathcal{M}(P) = 60°$.

The conditions in Theorem 1.1 only depend on the set of angles of P, not on their ordering around P, nor on the side lengths of P. Thus we immediately obtain the following solution to Problem C7 of [23].

Corollary 1.5. *If $\phi > 60°$ and P, P' are N-gons with the same set of angles (possibly in different orders around the boundary) then P has a ϕ-triangulation (or a ϕ-dissection) if and only if P' does.*

Finding triangulations with good angle bounds has a long history and many applications, e.g, see [16] or [62] for lists of algorithms, such as the finite element method, that work better with well formed meshes. Burago and Zalgaller's theorem from [19] was an element of their polyhedral version of the Nash embedding theorem, but it long remained unknown in the western computational geometry literature (partly for being written in Russian and partly for being a lemma in a topology paper). The first reference to it that I am aware of is [37] in 2004. In 1988 Baker, Grosse and Rafferty [5] independently proved that every polygon has a non-obtuse triangulation (all angles $\leq 90°$). This led to a large literature on algorithms for finding triangulations in various settings with guaranteed angle bounds, e.g., [8], [9], [10], [21], [16], [26], [31],

[41], [45], [47], [52], [56]. For a recent survey, see Chapter 29 of [35]. In 2002 Maehara [46] showed every non-obtuse triangulation can be converted to an acute one (with a comparable number of triangles), giving an alternate proof of the Burago-Zalgaller result. See also Yuan's paper [61]. A simpler approach was given by Saraf in [53].

Despite much effort devoted to finding triangulations with good geometry and optimal complexity, finding triangulations with optimal geometry has attracted less attention, at least when Steiner points are allowed. Triangulating the square with optimal angles is discussed by Gerver [33] and Eppstein [29], and Aronov, Asano and Funke [3], [4] give a polynomial time algorithm for maximizing the minimum angle when a fixed number of Steiner points are allowed (the degree of the work bound depending on the number of points added), but I do not know of other papers computing the optimal MinMax or MaxMin triangulation with arbitrary Steiner points. One possible reason may be the close connection to conformal mappings described below; it is hard to see how our proof of Theorem 1.1 could have been discovered using purely discrete geometric ideas.

Another reason may be the traditional focus on complexity. If the size of the triangulation is bounded by a function of $N = |V_P|$, independent of the geometry, then 90° is the best possible upper angle bound, e.g., if a $1 \times R$ rectangle with $R \gg 1$ is triangulated by $O(1)$ triangles, then there must be a small angle $\theta = O(1/R)$, and hence some large angle $\geq 90^\circ - \theta/2$. Thus the elements of an angle-optimal triangulation of an N-gon cannot be computed in polynomial time. This paper does not address the interesting question of finding efficient triangulations attaining the optimal bounds, but see Section 16 for some ideas on how this might be done. However, in Section 13 we will prove that the optimal angle bound $\Phi(P)$ is "easy" to compute.

Corollary 1.6. *$\Phi(P)$ can be computed in time $O(|V_P|)$.*

In 1992 Edelsbrunner, Tan and Waupotitsch [28] gave a $O(N^2 \log N)$ algorithm for minimizing the maximum angle of a triangulation of an N-gon without using Steiner points, and their result has not yet been improved, so far as I (or Edelsbrunner) know. Thus finding the optimal angle bound over all Steiner triangulations is faster than the best known algorithms for computing the optimal bound over the finitely many non-Steiner triangulations.

A similar situation regarding Steiner points occurs when decomposing a polygon into convex pieces: Chazelle and Dobkin [20] obtain a faster solution using Steiner points than is obtained by Keil and Snoeyink [38] without Steiner points. Their result, and the one given in this paper, runs counter to the general expectation that an optimization problem becomes harder by introducing Steiner points. For example, it is unknown whether a Steiner triangulation minimizing total edge length even exists for general polygons. See Section 16 for further remarks on this.

The main contribution of this paper is to show that (barring some well defined exceptions), the optimal angle bounds for triangulating with Steiner points are attained by some finite triangulation. The existence proof is a construction based on conformal mappings, which are often difficult to compute in practice, so the triangulations we produce are probably too computationally expensive for applications, especially as many excellent methods already exist, e.g., see [6], [11], [27], [31], [56]. However, Corollary 1.6 does give a fast and practical way to compute the optimal angle bound for any polygon, so it can be used to certify the output of any triangulation algorithm, or can be used to halt an iterative method once it is close enough to optimal. It would be interesting to test the optimality of various existing methods using Corollary 1.6; if they typically fail to approach the sharp bounds, then further research into optimizing the more computationally intensive conformal methods might be worthwhile.

To illustrate the relative ease of computing $\Phi(P)$, we will calculate it for several examples. Corollaries 1.7 to 1.10 are proven in Section 12.

Corollary 1.7. *For the regular N-gon, the sharp upper bound is $\Phi_N = 72^\circ$ except when $N = 3, 6, 7, 8, 9$; then $\Phi_N = 60^\circ$, 60°, $\frac{5}{7} \cdot 90^\circ$, 67.5°, and 70° respectively.*

Corollary 1.8. *Any 90°-polygon P has $\Phi(P) = 72^\circ$. The optimal triangulation may be taken with all interior vertices of degree six, except for two vertices of degree five.*

Here, a 90°-polygon is one where all the interior angles are multiples of 90°, e.g., all edges are either horizontal or vertical segments. Given P, let $\theta_{\min}, \theta_{\max}$ denote the minimum and maximum interior angles of P.

Corollary 1.9. *If T is a triangle with $\theta_{\min} \leq 36^\circ$, then $\Phi(T) = 90^\circ - \theta_{\min}/2$. If $\theta_{\min} > 36^\circ$, then $\Phi(T) = \min(72^\circ, \theta_{\max})$.*

When is a triangle an optimal triangulation of itself? Corollary 1.9 implies that if either (1) $\theta_{\max} \leq 72^\circ$, or (2) $\theta_{\min} \leq 36^\circ$ and T is isosceles, then $\Phi(T) = \theta_{\max}$, and hence T is its own MinMax optimal triangulation. In all other cases, $\Phi(T) < \theta_{\max}$, so there is some triangulation that is "better" than T itself.

The next result applies if P approximates a smooth curve (angles close to 180°).

Corollary 1.10. *If $\theta_{\min} \geq 144^\circ$, then $\Phi(P) = 72^\circ$. If $\theta_{\min} \geq 162^\circ$, then every triangulation angle may be taken in $[54^\circ, 72^\circ]$. If $144^\circ \leq \theta_{\min} \leq \theta_{\max} \leq 216^\circ$, then the triangulation may be chosen with six vertices of degree five (the rest have degree six).*

Note that 72° is frequently the sharp bound. This is partially explained by the fact that the set of N-gons with this optimal bound contains an open set in the space $\mathcal{P}_N$ of all simple N-gons (we put a topology on $\mathcal{P}_N$ by thinking of it as a subset of $\mathbb{C}^N$). For example, Corollary 1.10 shows the set of polygons with $\theta_{\min} > 144^\circ$ is such an open set. More precisely, we have the following result, proved in Section 14.

Corollary 1.11. *The map $P \to \Phi(P)$ is continuous. Thus $\{P \in \mathcal{P}_N : \Phi(P) \leq \phi\}$ is closed in $\mathcal{P}_N$, as is $\{P \in \mathcal{P}_N : \Phi(P) = \phi\}$. For large enough N, the latter set has non-empty interior iff $\phi = \frac{5}{7} \cdot 90^\circ$ or $\phi = 72^\circ$; for other values of ϕ it always has co-dimension ≥ 1.*

Suppose we wish to maximize the minimal angle of a triangulation, instead of minimizing the maximum angle? As noted earlier, the Delaunay triangulation of a point set maximizes the minimal angle without Steiner points; with Steiner points, angles arbitrarily close to 60° can be achieved for point sets. The constrained Delaunay triangulation does the same for triangulating polygons without Steiner points (see [42], [43]), and an algorithm using only interior Steiner points is presented in [48]. The methods of this paper can be used to maximize the minimum angle when triangulating a polygon P with arbitrary Steiner points. To state the result we introduce some more notation, analogous to that used in Theorem 1.1.

A ϕ-lower-triangulation means a triangulation with all angles $\geq \phi$, and we define $\widetilde{\Phi}(P)$ to be the supremum of ϕ so that P has a ϕ-lower-triangulation. For $0 < \phi < 60^\circ$ we define $\widetilde{I}(\phi) = [\phi, 180^\circ - 2\phi]$; any triangle having smallest angle ϕ must have all its angles inside $\widetilde{I}(\phi)$. Define a labeling L to be ϕ-lower-admissible if $\theta_v \in L(v) \cdot \widetilde{I}(\phi)$ where θ_v is the angle of P at $v \in V_P$. The curvature $\kappa(L)$ is defined just as before,

and $\widetilde{\mathcal{K}}(\phi)$ is the set of curvatures of ϕ-lower-admissible labelings. Also as before, $\widetilde{\kappa}(\phi)$ is the element of this set closest to 0 (equal to ∞ if no ϕ-lower-admissible labeling exists). The following result and its corollaries are proven in Section 15.

Theorem 1.12. *For $0 < \phi < 60°$, a polygon P has a ϕ-lower-triangulation iff*

(1) $0 < \phi \leq \frac{1}{7} \cdot 360° \approx 51.4286°$ *and* $\widetilde{\kappa}(\phi) < \infty$,
(2) $\frac{1}{7} \cdot 360° < \phi \leq 54°$, *and* $\widetilde{\kappa}(\phi) \geq 0$,
(3) $54° < \phi < 60°$, *and* $\widetilde{\kappa}(\phi) = 0$.

As before, there are a variety of consequences that follow; we list a few here.

Corollary 1.13. *$\widetilde{\Phi}(P)$ can be computed in time $O(|V_P|)$.*

Corollary 1.14. *If P has a ϕ-lower-triangulation, then it also has an acute ϕ-lower-triangulation.*

Corollary 1.15. *If $\theta_{\min} \leq 45°$, then $\widetilde{\Phi}(P) = \theta_{\min}$.*

Comparing Corollaries 1.3 and 1.15, we see that if P is a polygon with $\theta_{\min} = 45°$, then $\Phi(P) \leq 72°$ and $\widetilde{\Phi}(P) = 45°$. If P has at least one angle $\theta \in (72°, 90°)$, then any triangulation of P that attains the optimal upper bound $\Phi(P)$ must subdivide θ and hence has an angle strictly less than 45°, and hence $< \widetilde{\Phi}(\phi)$. This immediately gives the following consequence.

Corollary 1.16. *There exist polygons so that no triangulation attaining the optimal upper angle bound $\Phi(P)$ can achieve the optimal lower angle bound $\widetilde{\Phi}(P)$.*

Gerver [33] used conformal maps to transfer dissections from the unit disk to a polygon. In this paper, given a polygon P, we will construct a 60°-polygon P', together with a conformal map f between their interiors that defines a map between their vertices (in some cases, P will be replaced by a subdomain obtained by cutting a few "slits" in P). We then transfer a nearly equilateral triangulation from P' to P using f. More precisely, we map the triangulation vertices from P' to P, and connect the images by segments in P; we call these the "pushed forward" triangles (conformal images of the triangles themselves would have curved sides). A simple example is shown in Figure 4. The labeling shown in Figure 4 is 72°-admissible and has curvature 0, so $\kappa(72°) = 0$. Moreover, the reader can check that $\kappa(\phi) > 0$ for

$\phi < 72°$, hence $\Phi(P) = 72°$. As the mesh in Figure 4 gets finer, the largest angle tends to 72°, and we will show later that this limiting bound can be attained by modifying a sufficiently fine triangulation near the vertices (see Lemma 6.3).

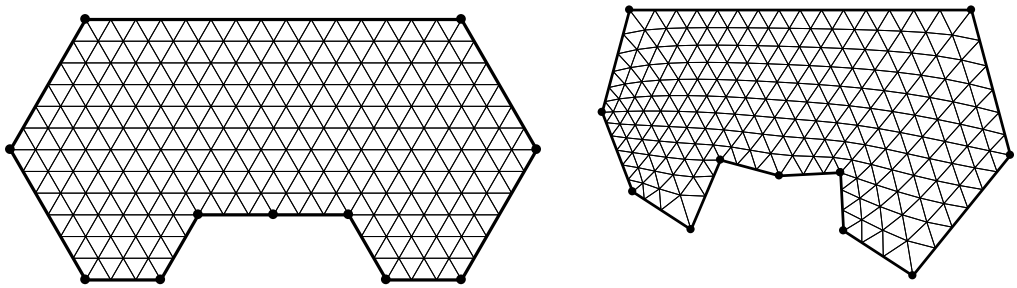

FIGURE 4. An equilateral triangulation of P' (left) and its conformal image P (angles: 270°, 126°, 96°, 126°, 105°, 105°, 144°, 144°, 80°, 262°, 162°). The maximum angle used here is $\approx 73.5205°$ and approaches 72° as the mesh gets finer; 72° is sharp by Theorem 1.1 and can be attained by modifying a sufficiently fine triangulation near the vertices.

We want P' to have a (nearly) equilateral triangulation, so we will assume it is a 60°-polygon. Note that such a triangulation of P' has all interior vertices of degree six. The angle of P' at the vertex corresponding to $v \in V_P$ is given by $60° \cdot L(v)$, where L is a labeling of V_P. Since the angles of P' sum to $(|V_P| - 2) \cdot 180°$, a short calculation shows that we must have $\kappa(L) = 0$. Given such a labeling of V_P, we will use the Schwarz-Christoffel formula to define P' and f. If we transfer a sufficiently fine and nearly equilateral triangulation from P' to P using f, the image will be close to a ϕ-triangulation of P if the labeling L is ϕ-admissible. Thus to start the construction, it seems that we need a ϕ-admissible labeling of P with zero curvature.

However, such a labeling need not exist. For example, suppose P is a pentagon with five equal angles of 108°. Theorem 1.1 (in particular, Corollaries 1.7 and 1.5) implies that $\Phi(P) = 72°$. However, the only 72°-admissible labels for a 108°-vertex are $\{2, 3\}$, so $\mathcal{K}(\phi) = \{1, \ldots, 6\}$ and so $\kappa(\phi) = 1 > 0$. This holds even if we add extra 180°-vertices to P (their possible labels are $\{3, 4, 5\}$). Therefore, any 72°-triangulation of P has positive curvature and thus it has at least one interior vertex of degree five (degree ≤ 4 implies an angle $\geq 90°$).

How can such a triangulation of P be a conformal image of a triangulation of P' that only has interior vertices of degree six? The answer is that we can choose f to conformally map the interior of P' into a subdomain of P obtained by cutting a slit in P. Two adjacent edges of P' are mapped to the two sides of the slit, and some boundary vertices of P' become interior vertices of P, thus the topology of the triangulation changes. See Figure 5. In general, up to $|\kappa(\Phi(P))|$ slits are used, introducing vertices of either degree five ($\kappa > 0$) or degree seven ($\kappa < 0$). We will prove the following sharp bounds for the number of such "exceptional" vertices in Section 11.

Corollary 1.17. *In Theorem 1.1, if a ϕ-triangulation $\mathcal{T}$ exists, then it can be constructed so that all interior vertices have degree six except that*

(1) *if $72^\circ \le \phi < 90^\circ$, then $\max(0, \kappa(\phi))$ vertices have degree five,*
(2) *if $\frac{5}{7} \cdot 90^\circ \le \phi < 67.5^\circ$, then $-\kappa(\phi)$ vertices have degree seven,*

For $67.5^\circ \le \phi \le 72^\circ$ there are $-\kappa(\phi)$ vertices of curvature -1, but these vertices may each be chosen either in the interior (degree seven) or on the boundary (degree four).

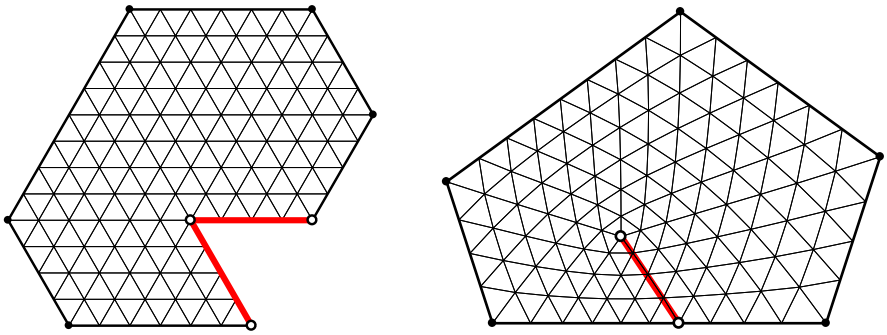

FIGURE 5. The edges adjacent to the 300°-vertex of P' are mapped to the two sides of the slit inside P. An interior vertex v of degree 5 is created. The slit is slightly curved to make the triangles on either side match up, although this is not easily visible (the actual slit lies slightly above the chord between its endpoints; total bending is about 3°).

The scheme outlined above encounters a number of difficulties, that we overcome using ideas from complex analysis. We list a few of these here, giving details later.

• **Conformal welding:** When we map boundary edges of P' to a slit in P, the images of certain boundary triangles in P' must match up across the slit in P, so

that the image will be a triangulation and not a dissection. This is only possible if the shape of the slit is carefully chosen so that arclength on each boundary segment maps to the same measure on the slit, i.e., we need $f(z) = f(w) \Rightarrow |f'(z)| = |f'(w)|$. This is a special case of a conformal welding problem, e.g., [12], [36], [51], and in our case it can be solved explicitly. The slit is generally not a segment, but may be close to one, as in Figure 5. If the slit were straight, then the Schwarz reflection principle would imply it lies on a line of symmetry for the triangles, which is not true here.

• **Riemann surfaces:** In cases where we introduce an interior vertex of degree seven, P' will need to have a boundary vertex of degree seven, i.e., P' has interior angle 420° at some vertex. Thus we necessarily consider "polygons" P' that are actually Riemann surfaces and not planar regions. See Figure 6.

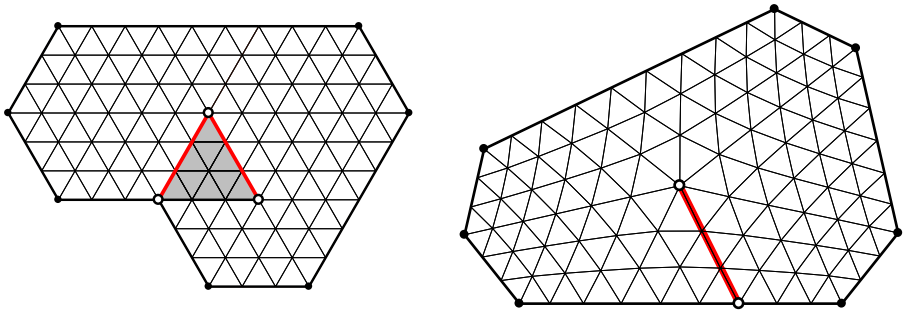

FIGURE 6. We triangulate an equal-angle heptagon using a Riemann surface with a 420°-vertex to insert a degree 7 vertex into the triangulation. The self-overlapping part of the surface is shaded.

• **Distortion estimates:** A conformal map f preserves interior angles infinitesimally, but to control our triangulation angles we shall need angle distortion estimates at positive scales, with bounds depending on the size of the triangle, its distance to the nearest vertex, and the ratio of the corresponding angles in P and P' at that vertex. Here we make use of the classical distortion theorems for conformal maps.

• **Harmonic measure:** Transferring a nearly equilateral triangulation from P' to P will allow us to approximate the optimal bounds, but to actually attain them, we need to also use triangulations of infinite sectors that arise as images of an equilateral triangulation of a 60°-sector under a power map z^α. Thus in some regions of P we utilize triangulations arising from two different conformal maps, and we use harmonic measure estimates to bound the difference between these conformal maps.

• **Quasiconformal mappings:** Given two triangulations of a region arising from different, but close, conformal maps, we merge the triangulations by using a partition of unity to interpolate from one conformal map to the other. The result is a quasiconformal map, and we shall use standard estimates on the angle distortion of such maps to control the angles of the interpolated triangulations. We also use such estimates to prove that any 60°-polygon has a nearly equilateral triangulation.

This paper arose from a related question asked by Florestan Brunck: given a planar triangulation with lower angle bound θ, does it have an acute refinement with upper angle bound strictly less than 90° and only depending on θ? In [14] I proved the answer is yes, by showing that every planar straight line graph (PSLG) Γ has a uniformly acute triangulation $\mathcal{T}$. This means that there is a universal $\theta_0 > 0$, independent of Γ, so that Γ has a conforming triangulation with all angles inside the fixed interval $[\theta_0, 90° - \theta_0/2]$, except for triangles that contain vertices v of Γ that have an interior angle $\theta_v < \theta_0$; these exceptional triangles are isosceles with angles in $[\theta_v, 90° - \theta_v/2]$. The proof in [14] uses a compactness argument, and does not give an explicit value for θ_0, but [13] shows we can take $\theta_0 = 30°$ in the special case of polygons. Dropping the requirement that exceptional triangles must contain a vertex of P permits an even smaller angle bound, and led me to formulate Theorem 1.1.

Section 2 gives an overview of the proof Theorem 1.1, and later sections provide the details. We end with some calculations, questions and remarks in Section 16.

Several figures are drawn using Toby Driscoll's SC-Toolbox package for MATLAB [24], an improved version of an earlier algorithm of Nick Trefethen [59] for computing Schwarz-Christoffel maps. I thank Toby for his assistance with the toolbox. I thank Joe Mitchell and Herbert Edelsbrunner for their helpful comments on an earlier version of this paper, and their encouragement to disseminate it in the computer science community. The results in this paper were announced at SODA 2022 [17], and the referees judging submissions provided many helpful suggestions. I am also very thankful to an anonymous referee who provided numerous suggestions for correcting the grammar and the mathematical exposition; these remarks greatly improved the paper.

2. Overview of the proof

The basic idea to introduce a class of polygons that have "nearly equilateral" triangulations (all angles close to 60°) and use conformal maps to transfer these triangulations to general polygons.

We will say that a simple polygon is an equilateral grid-polygon if its edges are contained in a grid of the plane consisting of congruent equilateral triangles, and its vertices are vertices of the grid. These are exactly the simple polygons that have a triangulation by equilateral triangles. See Figure 7.

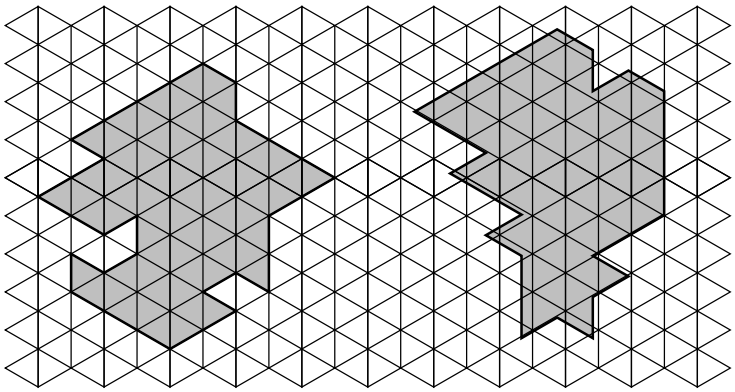

FIGURE 7. On the left is a equilateral-grid polygon, and on the right is a 60°-polygon.

It will be convenient to enlarge this class to the class of 60°-polygons, whose interior angles are all multiples of 60°. We will say that a polygon P has nearly equilateral triangulations if for any $\epsilon > 0$ it has a triangulation with all angles in $[60° - \epsilon, 60° + \epsilon]$ and that each vertex of P has a neighborhood in which the triangulation elements are actually equilateral (this is used to attain the desired angle bounds, instead of just approximating them). We will prove that every 60°-polygon has nearly equilateral triangulations in this sense; see Lemma 5.1. This lemma includes 60°-surfaces, i.e., simply connected Riemann surfaces R obtained by identifying 60°-polygons along matching edges. The boundary of R projects into the plane, possibly with self-intersections. Such surfaces arise as Schwarz-Christoffel images of the disk (see Section 10) when all the angles are multiples of 60°, but the map is not globally 1-to-1.

Suppose $f : \Omega' \to \Omega$ is a conformal mapping between the interiors of two polygons P' and P, and that f induces a bijection between vertices of P' and vertices of P.

(Below, we will often use P to refer to both the boundary curve and the interior domain, instead of using Ω for the latter; the meaning should always be clear from context.) Then f will only slightly perturb the angles of sufficiently small triangles in Ω', unless they are near vertices of P' (see Corollary 3.3). If v' is a vertex of P' with angle ψ that maps to a vertex v of P with angle θ, then any small triangle close enough to v' will have its interior angles distorted by at most θ/ψ (see Lemma 6.1).

The triangulations we construct will have all their angles between 36° and 72°, except for some triangles near vertices of P that may have angles less than 36°. Larger angles of P will be subdivided by the triangulation to give new angles that are all in the interval $[36°, 72°]$, and these sub-angles should each map to 60° under the conformal map from P to P'. In order to have this work out correctly, we need an angle θ in P to correspond to an angle $\psi = L(v) \cdot 60°$ in P' that satisfies

$$\frac{3}{5}\psi \le \theta \le \frac{6}{5}\psi. \tag{2.1}$$

The restrictions imposed by (2.1) are summarized by Table 1 and Figure 8. For example, if P has a vertex v with interior angle $\theta = 135°$, then the corresponding vertex v' in the 60°-polygon P' must have angle either 120° or 180°. Any other choice means that the triangles containing v' in the nearly equilateral triangulation of P' map to triangles with angles either less than 36° or larger than 72°.

θ range	allowable ψ
0–72	60
72–108	120
108–144	120, 180
144–180	180, 240
180–216	180,240, 300
216–288	240, 300, 360
288–360	300, 360

TABLE 1. Given an angle θ of P, this table gives the possible corresponding ψ's in P' needed to attain $\Phi(P) \le 72°$. Note that angles $\le 36°$ in P imply there are angles $\ge 72°$ in the triangulation.

Figure 8 plots $\cup_k k \cdot I(\phi)$ vertically above each value of ϕ. The result is a union of shaded triangles. P can have a ϕ-admissible labeling only if all its angles lie in the intersection of the shaded region and the vertical line through ϕ. For $72° \le \phi \le 90°$,

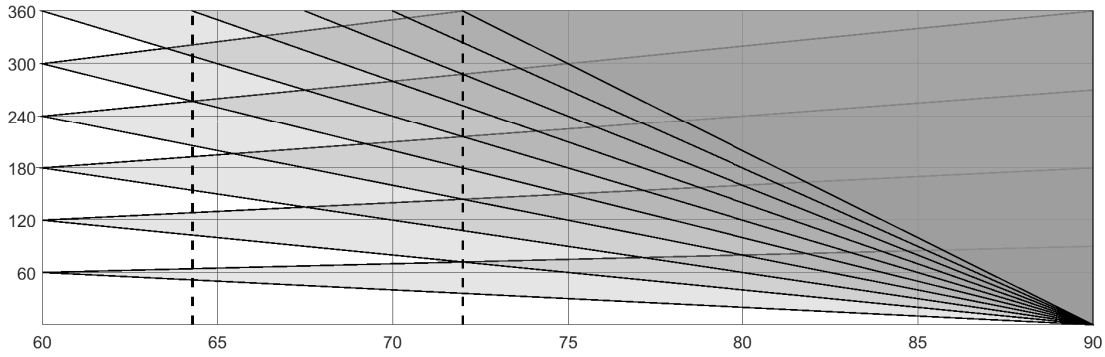

FIGURE 8. P has a ϕ-admissible labeling if and only if all its angles lie in the union of shaded triangles, on the vertical line through ϕ. The dashed vertical lines indicate where the transitions occur in Theorem 1.1, i.e., $\phi = \frac{5}{7} \cdot 90°$, and $\phi = 72°$.

$\cup_k k \cdot I(\phi) = [180° - 2\phi, \infty)$ so this condition only depends on the size of $\theta_{\min}$, and is equivalent to having a ϕ-triangulation. This observation is the reason why Corollary 1.3 follows from Case 1 of Theorem 1.1; we will explain this further in Section 10. For $\phi < 72°$, having a ϕ-triangulation requires all the angles of P to lie in this intersection (which is now disconnected), and we must also be able to choose the indices of the triangles containing these angles to satisfy certain linear constraints (the curvature conditions in Theorem 1.1).

Unfortunately, there are some polygons P whose vertices cannot be put into 1-1 correspondence with the vertices of a 60°-polygon so that they satisfy the restrictions in Table 1 and Figure 8. In general, the interior angles $\{\theta_1, \ldots, \theta_N\}$ of an N-gon must satisfy $\sum_k \theta_k = (N-2)180°$. When we assign image angle values $\{\psi_1, \ldots, \psi_N\}$ using (2.1) or Table 1, we need to have $\sum_k \psi_k = (N-2)180°$, but this is sometimes impossible. For example, if P is a square, then each of its four 90° angles would have to be assigned angle 120° in P', giving an angle sum $480° > 360°$. We can "fix" the angle discrepancy by adding extra vertices to the edges of P.

First suppose $\sum_k \psi_k < \sum_k \theta_k$. We add a new vertex v of angle 180° in an edge of P, and assign the corresponding vertex v' in P' the angle $240° \leq \frac{6}{5} \cdot 180°$. See Figure 9. Doing this increases the angle sum $\sum \theta_k$ by 180° but increases the angle sum $\sum \psi_k$ by 240°, decreasing the gap between them by 60°. Doing this several times we can clearly make the two sums match, as desired. Four equilateral triangles in P' touch

v', and they are mapped to four triangles in P touching v. They have angle 45° at v and the opposite angles are approximately 67.5° (some distortion may occur). Hence using this method can only give ϕ-triangulations with $\phi \geq 67.5°$. This is adequate to prove Case 1 of Theorem 1.1 but a more elaborate construction is needed to prove Cases 2 and 3.

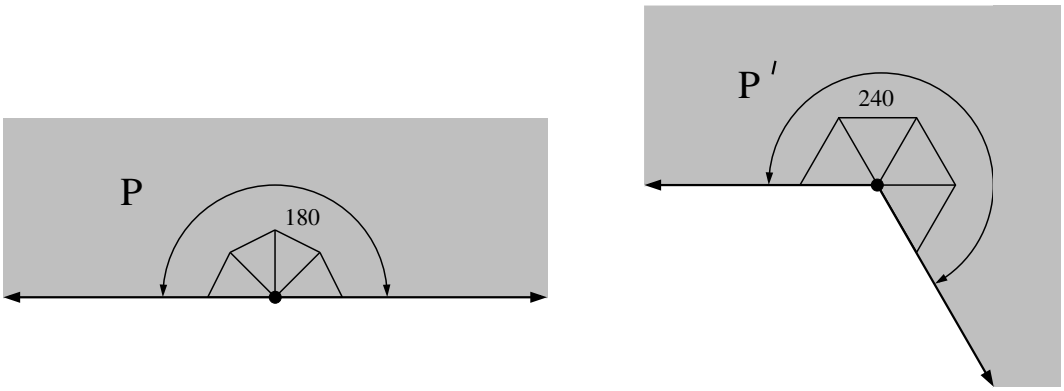

FIGURE 9. Our first trick for increasing the ψ-sum relative to the θ-sum is to pair a 180°-vertex in P with a 240°-vertex in P'. The conformal map locally looks like $z^{3/4}$, and maps a 60° sub-angle to 45°. A triangle containing this angle also contains an angle ≥ 67.5.

In Case 2 of Theorem 1.1 we want to get the angle 67.5° down to $\frac{5}{7} \cdot 90° \approx 64.2857$. We will do this by using a triangulation of a slit half-plane based on transferring an equilateral triangulation from a polygonal Riemann surface that has a 420° angle in its boundary. The idea is shown in Figure 10; the details will be given in Section 8. The Riemann surface R is built by attaching two planar domains as shown on the left side of Figure 22. R has a 1-1 projection onto a sector of angle 240°, except for the darker triangle where it is 2-1. Traversing the boundary, we encounter angles 60°, 420° and 120°. The 420°-vertex belongs to seven triangles in R and will map to a degree seven interior vertex in the final triangulation.

The two segments adjacent to the 420°-vertex are mapped to a slit in P where the angles are 60°, 180° and 120°. The worst distortion comes from mapping the 420°-vertex in P' to the 360°-vertex in P (the tip of a slit). Locally the map looks like $z^{6/7}$, that maps each 60° sub-angle to $\frac{6}{7} \cdot 60° = \frac{4}{7} \cdot 90° \approx 51.4286$. A triangle with this angle must also contain an angle $\geq \frac{5}{7} \cdot 90° \approx 64.2857$, which is where this angle in Theorem 1.1 comes from. Note that the two finite boundary segments of R are

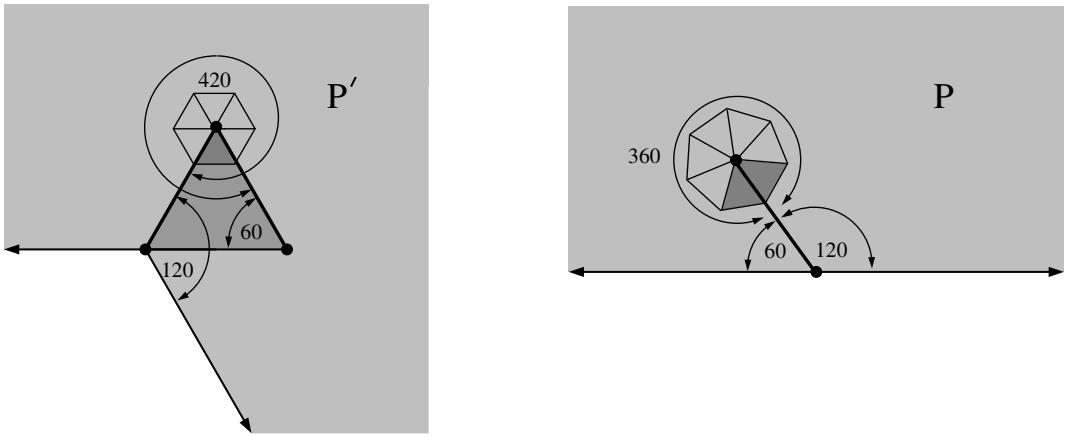

FIGURE 10. We cut a slit in the upper half-plane at angle 60°. This models a neighborhood of a 180°-vertex on the boundary of P. The angles we observe tracing the outline of the slit are: 60°, 360° and 120°. The triangulation near this slit will correspond to an equilateral triangulation of a Riemann surface R with angles 60°, 420° and 120°, pictured at right. R is a 1-1 cover of a 240°-sector, except for the darker triangle where it is 2-1.

both mapped to the slit in P, so triangulation edges along these two sides of R must map to matching edges along the slit. This requires that the conformal map sends the length measures on the two segments to the same measure on the slit (but not necessarily length measure). See Figure 23.

If $\sum_k \psi_k > \sum_k \theta_k$ we use a slightly easier variant of the 420°-trick that we call the "120°-trick". This involves mapping a slit half-plane to a 120°-sector with a triangle removed, as shown in Figure 11. Traversing the boundary of the slit half-plane we encounter angles 60°, 360°, and 120°, but traversing the boundary of the modified 120°-sector we encounter 60°, 300° and 120°, so the ψ-sum decreases by 60° relative to the θ-sum. As in the 420°-trick, the shape of the slit can be chosen so that points on the two identified segments are paired according to their distance from the 300°-vertex. In that case, an equilateral triangulation of the modified sector will map to a triangulation of the half-plane. Note also that exactly one degree five vertex is created in the triangulation, located at the tip of the slit. See also Figure 20.

Sections 3-8 will provide the details of the various constructions sketched above. The proof of Theorem 1.1 and its corollaries starts in Section 9.

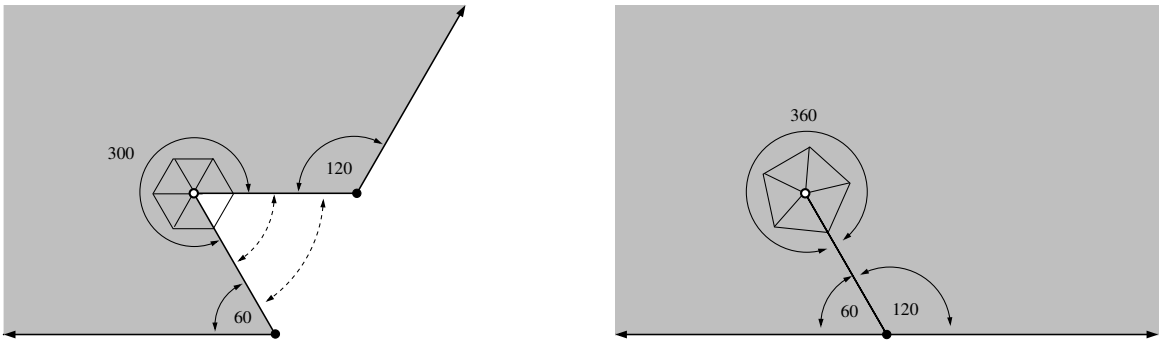

FIGURE 11. Take a 120°-sector and cut out an equilateral triangle (left). Conformally map this region to a slit half-plane (right). The two edges adjacent to the 300°-vertex are mapped to opposite sides of the (slightly) curved slit, and points on these edges equidistant from this vertex are identified. This implies that an equilateral triangulation on the left pushes forward to a triangulation on the right.

3. The distortion theorem

We let $D(z,r) = \{w : |z-w| < r\}$, $\mathbb{D} = D(0,1)$ and $\mathbb{T} = \partial\mathbb{D} = \{z : |z| = 1\}$. In this paper, a conformal map always refers to a 1-to-1 holomorphic mapping. Thus, to us, a conformal map is both angle and orientation preserving. By the Riemann mapping theorem, there is a conformal map from $\mathbb{D}$ onto any proper, simply connected subdomain of the plane, in particular, the interior of any bounded polygon. The same holds for any simply connected Riemann surface that is not homeomorphic to the 2-sphere or conformally equivalent to the plane; this is true for all the Riemann surfaces we shall consider in this paper. For Jordan domains, the conformal map extends to a homeomorphism between the boundaries; this will be the case for the all the polygonal domains and surfaces that we consider in this paper. The conformal map is unique if we specify the image of 0 and of one boundary point. For a conformal map from $\mathbb{D}$ onto a region Ω bounded by an N-gon P, the N preimages of the vertices on $\mathbb{T}$ are called the prevertices.

We start by recalling a fact from complex analysis that we will use below (this is a special case of the Borel-Carathéodory theorem).

Lemma 3.1. *If g is holomorphic on $\mathbb{D}$ and $g(0) = 0$ then*

$$\max_{|z|<1/2} |g(z)| \le 2 \max_{|z|<1} |\mathrm{Re}(g(z))|.$$

Proof. Without loss of generality we may assume that $\mathrm{Re}(g) < 1$ on $\mathbb{D}$, so that g maps the disk into the half-plane $H = \{x + iy : x < 1\}$. If $\tau(z) = z/(2-z)$ is a Möbius transformation that takes H to $\mathbb{D}$ and fixes 0, then by the Schwarz lemma, $|\tau(g(z))| \le |z|$. Therefore g maps $\mathbb{D}$ into $\tau^{-1}(D(0, \frac{1}{2})) \subset D(0, \frac{1}{2})$. □

By definition, a conformal map f on a domain Ω preserves angles infinitesimally. We will need to show they almost preserve angles in triangulations in the following way. When we map a triangulation by a conformal map, we don't take the image $f(T)$ of each triangle T; this would have curved sides. If $T = \Delta ABC \subset \Omega$ has vertices A, B, C, we define the pushed forward triangle $f^*(T) = \Delta f(A)f(B)f(C)$, i.e., the triangle with vertices $f(A), f(B), f(C)$. See Figure 12. We wish to prove that pushing forward small triangles in Ω by conformal maps alters the angles by as little as we wish, except near the vertices.

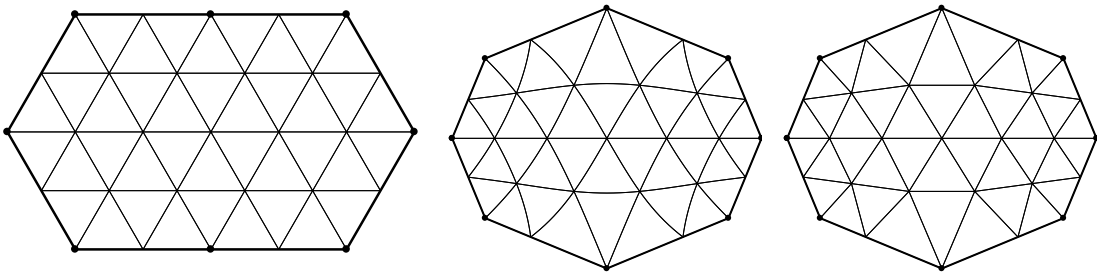

FIGURE 12. An equilateral triangulation (left), the actual conformal images of the triangles (center), and the pushed forward triangles (right) where vertex images are connected by segments.

Lemma 3.2. *If f is a conformal map on a disk $D(z, r)$, $0 < \delta < 1/4$, and $T = \Delta ABC$ is triangle inside $D(z, \delta r)$, then the triangle $f^*(T) = \Delta f(A)f(B)f(C)$ has angles that are within $O(\delta)$ of the corresponding angles of T.*

Proof. Since pre or post-composing f by a similarity does not change the angles of $f^*(T)$, we may assume $z = 0$, $r = 1$, $f(0) = 0$ and $f'(0) = 1$. The distortion theorem for conformal maps (e.g., Theorem I.4.5 of [32]), says that

$$\frac{1 + |z|}{1 + |z|^3} \le |f'(z)| \le \frac{1 + |z|}{1 - |z|^3}.$$

Thus $\log|f'(z)| \le \log(1+|z|) - \log(1-|z|^3)$. Using Lemma 3.1, and the facts that $\log(1+x) \le x$ and $\log 1/(1-x) \le 1+2x$ for $x \in [0, \frac{1}{2}]$, implies

$$\begin{aligned}\max_{|z|<\delta} |\arg(f'(z))| &\le 2\max_{|z|<2\delta} \log(1+2|z|) + 2\log\frac{1}{1-8|z|^3} \\ &\le 2\max_{|z|<2\delta} 2|z| + 32|z|^3 \\ &\le 4\delta + 64\delta^3 \le 8\delta\end{aligned}$$

if $\delta \le 1/4$. Therefore, inside $D(0,\delta)$ any segment S is mapped to a smooth curve all of whose tangents are within 8δ of being parallel of S. Hence the chord connecting the endpoints of $f(S)$ is within 8δ of being parallel to S, and so the angles of $f^*(T)$ are within 16δ of the corresponding angles of T. □

Next, we quantify the fact that, except near the corners, a conformal map between polygons alters triangle angles very little.

Corollary 3.3. *Suppose f is a conformal map between the interiors of two polygons P and P' that maps vertices to vertices. Suppose V_P is the vertex set of P, Ω is the interior of P, and that $\{D_v\}_{v\in V_P}$ are disjoint disks around each vertex v. Define $\Omega_0 = \Omega \setminus \cup_{v\in V_P} D_v$ and suppose $T \subset \Omega_0$ is a triangle. Then for every $\epsilon > 0$ there is a $\delta > 0$ so that f changes the angles of T by less than ϵ if* $\operatorname{diam}(T) < \delta$.

Proof. Let $r > 0$ be the distance from Ω_0 to V_P and let $s > 0$ be the minimal distance between any two connected components of $P \setminus \cup_{v\in V_P} D_v$. If $z \in \Omega_0$ and $t = \frac{1}{2}\min(r,s)$, then we claim f extends to be conformal on the disk $D_1 = D(z,t)$. If $D_1 \subset \Omega_0$ this is obvious. Otherwise, D_1 does not hit any vertex of P and hits at most one edge e of P. Suppose $w \in D_1 \cap e$. Then $D_1 \subset D_2 = D(w, 2t)$. Since the edge e of P maps to an edge of P', the Schwarz reflection principle says f can be extended to be conformal on all of D_2, hence on D_1, proving the claim.

Therefore, if $T \subset \Omega_0$ has diameter δ, then it is contained in a disk of radius t where f is conformal and hence the angles of T are distorted by at most $O(\delta/t)$. Since t is fixed, this is as small as we wish, if δ is small. □

4. Approximation in finite sectors

A K-quasiconformal map h of the plane is a homeomorphism of the plane to itself that is absolutely continuous on almost all lines and whose complex dilatation

$\mu = h_{\bar{z}}/h_z$ satisfies $\|\mu\|_\infty \le k < 1$ where $k = (K-1)/(K+1)$. Recall $h_z = \frac{1}{2}(\frac{\partial h}{\partial x} - i\frac{\partial h}{\partial y})$ and $h_{\bar{z}} = \frac{1}{2}(\frac{\partial h}{\partial x} + i\frac{\partial h}{\partial y})$. At the points where f is differentiable, the derivative is a linear map sending a circle to an ellipse, and this definition implies the eccentricity of the image ellipse (i.e., ratio of the major axis to the minor axis) is bounded by K. A map is quasiconformal if it K -quasiconformal form some $K < \infty$. See [1] or [44] for the basic properties of quasiconformal mappings. One such property is that pre or post-composing a K-quasiconformal map by a conformal map gives another K-quasiconformal map: a simple calculation with the chain rule shows the phase of the dilatation may change, but its absolute value does not. An important property of K-quasiconformal maps $\mathbb{C} \to \mathbb{C}$ is that they form a compact family when normalized to fix two points, usually taken to be 0 and 1. Also, a 1-quasiconformal map is conformal, so a 1-quasiconformal map of the plane to itself must be linear. These facts imply the following.

Lemma 4.1. *For any $\delta > 0$, there is a $\epsilon > 0$ so that if f is a $(1+\epsilon)$-quasiconformal map from $\{|z| < 1/\epsilon\}$ into $\mathbb{C}$, then $|f(z) - z| \le \delta |f(0) - f(1)|$ on $\mathbb{D}$.*

Proof. Suppose not. Since pre and post-composing by similarities (these are conformal) does not change the quasiconformal bound, we may assume there is a sequence of K_n-quasiconformal maps on $\{|z| < n\}$ into $\mathbb{C}$ with $K_n \to 1$, that fix both 0 and 1, but so that each map moves some point of $\mathbb{D}$ by more than δ. By compactness of normalized K-quasiconformal maps, any subsequence has a uniformly convergent (on $\mathbb{D}$) subsequence to a conformal linear map, that must be the identity. This contradicts the assumption that every map moves some point by at least δ. □

Using the Law of Sines, we can deduce that under the same hypotheses the push forward of any triangle $T \subset \mathbb{D}$ has its angles changed by at most a factor of $O(\delta)$.

Given a Jordan domain Ω, a point $z \in \Omega$ and a Borel set $E \subset \partial\Omega$, the harmonic measure, $\omega(z, E, \Omega)$ is the Lebesgue length of $f^{-1}(E) \subset \mathbb{T} = \partial\mathbb{D}$, where f is a conformal map $f : \mathbb{D} \to \Omega$ with $f(0) = z$. More intuitively, it is the probability that a Brownian motion started at z first hits $\partial\Omega$ in the set E, and it is the value at z of the harmonic function u on Ω that has boundary value 1 on E and zero elsewhere (appropriately defined). A similar definition works for simply connected domains, but in this case the conformal map $f : \mathbb{D} \to \Omega$ may not have a continuous

boundary extension, and much extra care is needed to define $f^{-1}(E)$ for $E \subset \partial\Omega$. In this paper, we only need to deal with Jordan domains, where the conformal map extends homeomorphically to the boundary. The text [32] of Garnett and Marshall is a comprehensive treatment of harmonic measure on planar domains, and includes all the results we shall use below.

An infinite sector is a region congruent to $S(\theta) = \{re^{i\phi} : r > 0, -\theta/2 < \phi < \theta/2\}$. The boundary consists of two infinite rays meeting at its vertex and the angle of the sector is the interior angle θ made by these rays. A finite sector is a region congruent to $S(\theta) \cap D(0,t)$ for some $t > 0$ and $\theta \in (0, 360°]$. For $r > 1$, let $A(r) = \{z : 1/r < |z| < r\}$. An annular sector is a region congruent to $S(\theta, r) = S(\theta) \cap A(r)$. Let $z_0 = 1$ be the center of the circular arc $\gamma = S(\theta) \cap \mathbb{T}$ and let $z_1 = e^{i\theta/2}$ be one endpoint of γ.

Lemma 4.2. *With notation as above, suppose Ω_1 and Ω_2 are Jordan domains so that for $k = 1, 2$, $\Omega_k \cap A(r)$ both have connected components equal to $S(\theta, r)$. Suppose $F : \Omega_1 \to \Omega_2$ is the conformal map that fixes z_0 and z_1. As $r \to \infty$, F converges uniformly to the identity on $S(\theta, 2)$.*

Proof. It is enough to take $\Omega_2 = S(\theta, r)$; in general, the conformal map $\Omega_1 \to \Omega_2$ can be written as the composition of conformal maps $\Omega_1 \to S(\theta, r) \to \Omega_2$, so it is enough to show each of these is close to the identity on $S(\theta, 2)$.

Let $f : \Omega_1 \to \mathbb{D}$ be the conformal map sending z_0 to 0 and z_1 to i. See Figure 14. By standard estimates, e.g., a version of the Ahlfors distortion theorem, such as Theorem IV.6.2 of [32], the harmonic measure of the circular arcs of $S(\theta, r) \cap \partial A(r)$ with respect to z_0 is $O(r^{-\pi/\theta})$. This tends to zero as $r \nearrow \infty$. Since harmonic measure is a conformal invariant, the images of these two curves under f have the same harmonic measures with respect to 0. The following lemma implies that they also have Euclidean diameter bounded by $O(r^{-\pi/\theta})$.

Lemma 4.3. *Let $\gamma \subset \mathbb{D}$ be a cross-cut of $\mathbb{D}$ (an arc in $\mathbb{D}$ with both endpoints on $\mathbb{T}$). Then* $\operatorname{diam}(\gamma) \le C\omega(0, \gamma, \mathbb{D} \setminus \gamma)$ *for some $C < \infty$ independent of γ.*

Proof. Let $\gamma^* = \{|z|/z : z \in \gamma\}$ be the radial projection of γ into the unit circle $\mathbb{T}$. By the radial version of Hall's lemma (e.g., Exercise III.20.d of [32]) there is an absolute constant $C > 0$ so that

$$\omega(0, \gamma, \mathbb{D} \setminus \gamma) \ge C\omega(0, \gamma^*, \mathbb{D}).$$

Since γ is connected, γ^* is a sub-arc of $\mathbb{T}$, so its harmonic measure from 0 equals its length divided by 2π. Thus the radial projection of γ has length bounded by a multiple of its harmonic measure, i.e., it is bounded by $O(r^{-\pi/\theta})$.

Similarly, if we let $\widetilde{\gamma} = \{|z| : z \in \gamma\}$ be the circular projection of γ into $[0, 1)$, then Beurling's projection theorem (Theorem III.9.2 in [32]) says that

$$\omega(0, \gamma, \mathbb{D} \setminus \gamma) \geq \omega(0, \widetilde{\gamma}, \mathbb{D} \setminus \widetilde{\gamma}).$$

Since γ is a cross-cut, its circular projection is an interval of the form $[1-\epsilon, 1)$. The domain $\mathbb{D} \setminus [1-\epsilon, 1)$ can be conformally mapped to $\mathbb{D}$ by a composition of Möbius transformations and power maps

$$f(x) = \tau^{-1}\left(\sqrt{\tau^2(z) - \tau^2(1-\epsilon)}\right),$$

where $\tau(z) = (1-z)/(1+z)$ map the disk to the right half-plane. See Figure 13.

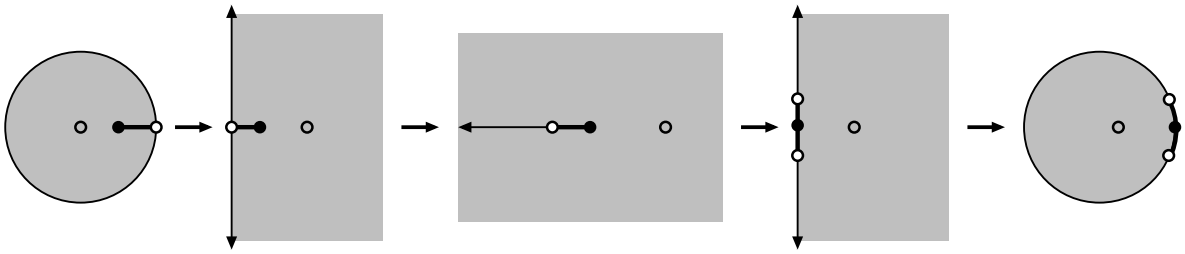

FIGURE 13. Estimating the harmonic measure of the slit in a slit disk. The slit disk can be conformally mapped to the disk by an explicit composition of Möbius transformations, power maps and a translation. A slit of length ϵ maps to an arc of length $\approx 2\epsilon$ and the origin moves by $\approx 2\epsilon$. Thus the harmonic measure of the slit is $\approx 2\epsilon$.

Simple estimates show that the segment $[1-\epsilon, 1)$ gets mapped to a sub-arc I of $\mathbb{T}$ of length $2\epsilon + O(\epsilon^2)$ centered at 1, and that 0 is moved to right by $2\epsilon + O(\epsilon^2)$. The harmonic measure of I with respect to the new base point is clearly at least ϵ, so we can deduce $\operatorname{diam}(\widetilde{\gamma}) = \epsilon = O(\omega(0, \gamma, \mathbb{D} \setminus \gamma))$. A set with both its radial and circular projections having diameter $\leq \epsilon$, itself has diameter less than 2ϵ, so the claim that $\operatorname{diam}(\gamma) = O(\omega((0, \gamma, \mathbb{D} \setminus \gamma))$ is now proved. □

Now back to the proof of Lemma 4.2. Let $E_r = f(\Omega \setminus S(\theta, r)) \subset \mathbb{D}$, and let E_r^1 and E_r^2 denote its two components. The arguments above say the diameters of these components are each $O(r^{-\pi/\theta})$, and hence they shrink to zero as r increases to ∞.

Moreover, as $r \nearrow \infty$, symmetry across $\mathbb{R}$ implies the two radial segments making up $\partial S(3) \cap \partial\Omega$ both have harmonic measure (with respect to z_0) approaching $1/2$. Similarly, reflection across $\mathbb{T}$ shows the four sub-segments inside and outside $\mathbb{T}$ all have harmonic measures approaching $1/4$. Since $f(z_1) = i$ and E_r^1 and E_r^2 both have small diameters, this implies they are respectively contained in small disks around ± 1. See Figure 14.

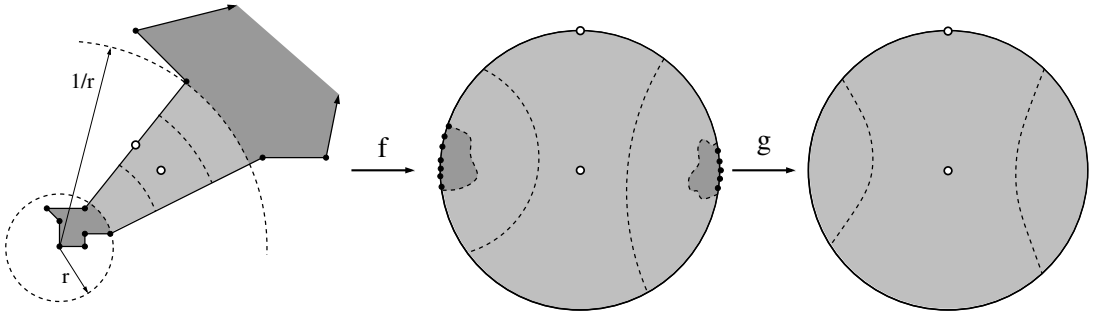

FIGURE 14. The conformal map from Ω_1 to $S(\theta, r)$ can be written as a composition $F = f^{-1} \circ g \circ f$ where $f : \Omega_1 \to \mathbb{D}$ and g is a map of $\mathbb{D} \setminus f(\Omega_1 \setminus S)$ to $\mathbb{D}$. The components of $f(\Omega_1 \setminus S(\theta))$ have small diameter as $r \nearrow \infty$, so both g and $F = f^{-1} \circ g \circ f$ are close to identity maps.

Let g_r be the conformal map from $\mathbb{D} \setminus E_r$ to $\mathbb{D}$ that fixes 0 and i. Let F_r be the reflection of E_r over the unit circle. By Schwarz reflection, g extends to a conformal map on $W_r = \mathbb{C} \setminus \overline{E_r \cup F_r}$. Thus if $\delta > 0$, and r is sufficiently large (depending on δ), then g_r is conformal on $W_\delta = \mathbb{C} \setminus (D(-1, \delta) \cup D(1, \delta))$ and $g_r(W_\delta)$ omits $-1, 1, \infty$. Hence this family of maps is normal and any subsequence converges uniformly on compact subsets of W_δ to a conformal map on W_δ. Taking a sequence of δ's converging to zero and diagonalizing, we get that every subsequence of g_{r_k} with $r_k \nearrow \infty$ contains a subsequence that converges uniformly on compact subsets of $W_0 = \mathbb{C} \setminus \{-1, 1\}$ to a conformal map of W_0 that fixes 0 and i. This map extends to be 1-1 and holomorphic on the plane, hence linear, hence the identity. Since the limit is unique, we deduce that the whole family $\{g_r\}$ converges uniformly on compact subsets of W_0 to the identity.

Since $f(S(\theta, 2))$ is pre-compact in $\mathbb{C} \setminus \{-1, 1\}$, we see that g_r is defined on this set for large enough r, and that it converges uniformly to the identity there. Thus

$F = f^{-1} \circ g \circ f : \Omega_1 \to S(\theta, r)$ is well defined, conformal, fixes z_0 and z_1, and tends to the identity uniformly on $S(\theta, 2)$ as $r \nearrow \infty$, proving the lemma. □

Recall that $A(r) = \{z : \frac{1}{r} < |z| < r\}$ and suppose that Ω_1 and Ω_2 are Jordan domains, and that both $\Omega_1 \cap A(3)$ and $\Omega_2 \cap A(3)$ have connected components equal to $S(\theta, 3)$. Let Ω_1^* be the component of $\Omega_1 \setminus 3\mathbb{T}$ that contains $S(\theta, 3)$ and let Ω_2^* be the component of $\Omega_2 \setminus \frac{1}{3}\mathbb{T}$ that contains $S(\theta, 3)$. We will say Ω_1 and Ω_2 as above are "compatible" if $\overline{\Omega_1^*} \cap \overline{\Omega_2^*} = \overline{S(\theta, 3)}$. In this case, $\Omega^* = \Omega_1^* \cup \Omega_2^*$ is a Jordan domain.

Lemma 4.4. *Suppose Ω_1 and Ω_2 are compatible in the sense just defined. Suppose f_k is conformal on Ω_k, $k = 1, 2$ and $\sup_{S(\theta,3)} |f_1 - f_2| < \epsilon$. If I is either one of the two radial segments of $\partial S(\theta, 3)$, suppose that f_1, f_2 both map I into the same line. Let $\eta : [0, \infty) \to [0, 1]$ be smooth with $\eta(t) = 0$ if $t < 1/2$ and $\eta(t) = 1$ if $t > 2$. Then*

$$g(z) = \begin{cases} f_1(z), & z \in \Omega_1^* \setminus S(\theta, 3) \\ f_2(z), & z \in \Omega_2^* \setminus S(\theta, 3) \\ f_1(z)(1 - \eta(|z|)) + f_2(z)\eta(|z|), & z \in S(\theta, 3) \end{cases}$$

is quasiconformal on Ω^* with complex dilatation bounded by $O(\epsilon)$ on $S(\theta, 3)$ and is equal to zero elsewhere.

Proof. By the assumption on the boundaries, both f_1, f_2 can be extended by reflection across the radial boundary segments of $\partial S(\theta, 3)$, and hence the Cauchy estimates are valid with a uniform radius at every point of $\partial S(\theta, 2)$. Therefore $|f_k'(z)| \simeq 1$ on $S(\theta, 2)$ for $k = 1, 2$. It also follows that

$$|f_2'(z) - f_1'(z)| = O(|f_2(z) - f_1(z)|) = O(\epsilon).$$

Next we estimate the dilatation $\mu = \partial_{\bar{z}} g / \partial_z g$. First,

$$\begin{aligned} \partial_z g(z) &= f_1'(z)(1 - \eta(|z|)) - f_1(z)\partial_z \eta(|z|) + f_2'(z)\eta(|z|) + f_2(z)\partial_z \eta(|z|) \\ &= f_1'(z) + (f_2'(z) - f_1'(z))\eta(|z|) + (f_2(z) - f_1(z))\partial_z \eta(|z|) \\ &= f_1'(z) + O(\epsilon) \simeq 1, \end{aligned}$$

because $|\eta|, |\nabla \eta| = O(1)$ (recall η is a fixed smooth function). Since $\partial_{\bar{z}} f = 0$ for holomorphic functions f,

$$|\partial_{\bar{z}} g(z)| = |(f_2(z) - f_1(z))\partial_{\bar{z}} \eta(|z|)| = O(\epsilon).$$

Thus $|\mu_g| = |\partial_{\bar{z}} g / \partial_z g| = O(\epsilon)$ as desired. □

The same argument proves the following, slightly simpler, version where we assume the maps are defined on a common disk, instead of a sector. This version will be used to merge triangulations near tips of slits in the 120°-trick (see Section 7) and the 420°-trick (see Section 8) .

Lemma 4.5. *Suppose Ω_1, Ω_2 are Jordan domains and that $D(0,r) \subset \Omega_1 \cap \Omega_2$ for some $r > 4$. Suppose $f : \Omega_1 \to \Omega_2$ is conformal and $f(0) = 0$, $f'(0) = 1$. Let $\eta : [0,\infty) \to [0,1]$ be smooth with $\eta(r) = 0$ if $r \le 1/2$ and $\eta(r) = 1$ if $r \ge 2$. Then*

$$g(z) = \begin{cases} z, & |z| \le 1/2, \\ f(z), & |z| \ge 2, \\ z(1-\eta(|z|)) + f(z)\eta(|z|), & 1/2 < |z| < 2 \end{cases}$$

is quasiconformal from Ω_1 to Ω_2 with complex dilatation bounded by $O(1/r)$ as $r \nearrow \infty$.

Proof. The proof is almost identical to the proof of Lemma 4.4, except that we have to verify that $|f(z) - z| = O(1/r)$ if $|z| \le 2$. By considering $g(z) = f(rz)/r$ it suffices to show that if g is conformal on the disk, $g(0) = 0$ and $g'(0) = 1$ then $|g(z) - z| = O(1/r^2)$ on the disk or radius $2/r$. However, this follows from the classical estimate $|a_2| \le 2$ (or use Theorem I.4.5 of [32]). □

5. 60°-surfaces have nearly equilateral triangulations

As noted in the introduction, not every 60°-polygon P has an equilateral triangulation, but in this section we will prove that they all have nearly equilateral triangulations. Recall that this means that for any $\epsilon > 0$, there is a triangulation of P with all angles within ϵ of 60° and that all angles are equal to 60° in some neighborhood of each vertex (the neighborhood may depend on the triangulation). Also recall that we need this result for both planar polygonal regions and Riemann surfaces with polygonal boundaries.

Lemma 5.1. *Every 60°-surface P has nearly equilateral triangulations.*

Proof. We refer to the boundary curve of a 60° Riemann surface R as P, although it need not be a simple planar polygon. However, it does project to a planar N-gon, possibly with self-intersections. By rotating, we may assume the sides of this curve are parallel to lines in the usual equilateral grid in $\mathbb{C}$ (with one side of each triangle parallel to the vertical axis). Rescale the grid to have a small side length δ, and

consider the union of triangles compactly contained in the surface R that project onto elements of the δ-grid. When δ is sufficiently small, this union forms a simply connected sub-surface R' with boundary curve P' that is also a 60°-surface and also has N vertices. Each edge of P' corresponds to a parallel edge of P. See Figure 15. If we fix a conformal map of $\mathbb{D}$ to R, then by taking δ small enough, we can choose a conformal map onto R' so that the corresponding conformal prevertices on $\mathbb{T}$ (recall these are the preimages of a conformal map from the unit disk to the surface R') can be chosen to approximate the prevertices of P as closely as we wish.

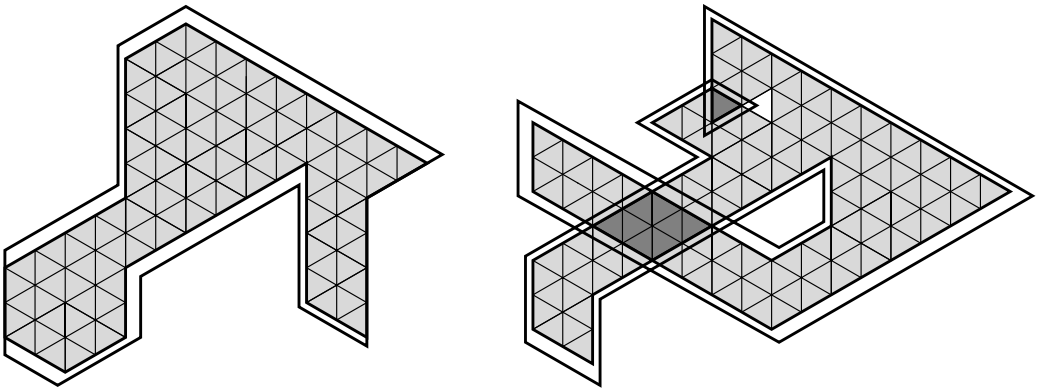

FIGURE 15. Two examples of approximating a 60° surface (white) by a union of equilateral triangles (shaded). On the left is simple polygon and on the right a Riemann surface. Overlaps of the surface with itself have darker shading.

Thus if the minimal distance between prevertices of P on $\mathbb{T}$ is $d > 0$, then given any $\epsilon > 0$ we may assume P' has exactly one prevertex within $\epsilon \cdot d/10$ of each prevertex of P. The following lemma implies there is a $(1+O(\epsilon))$-quasiconformal map Φ of the unit disk to itself that sends the prevertices of P' to the prevertices of P.

Lemma 5.2. *Suppose $\{z_j\}_1^n \subset \mathbb{T}$ are all at least distance $d > 0$ apart. Suppose $\{w_j\}_1 \subset \mathbb{T}$ satisfies $\max_{1\le j\le n} |w_j - z_j| < \epsilon d < d/4$. Then there is a $(1 + O(\epsilon))$-quasiconformal map φ so that $\varphi(w_j) = z_j$ for $j = 1, \dots n$, $\varphi(z) = z$ for all $|z| < 1-d$, and $\varphi(z)$ is conformal inside $D(z_j, \epsilon d)$ for $j = 1, \dots, n$.*

Proof. Let D_j the disk of radius $d/2$ around z_j. By assumption these disks are disjoint. Outside these disks define $\varphi(z) = z$. To define the map inside $\mathbb{D} \cap D(z_j, d/2)$ it is convenient to move to the upper half-plane via a Möbius transformation τ that sends

$z_j \to 0$, $-z_j \to \infty$, and $0 \to i$. Then $D_j \cap \mathbb{D}$ maps to a half-disk centered at 0 and radius $\frac{1}{2}d + O(d^2)$. The point w_j maps to a point x_j on the real axis with $|x_j| < 2\epsilon d$, if d is sufficiently small. The interpolating QC map can be given by a piecewise affine map between the triangulations shown in Figure 16. The angles all change by less than a factor of $O(\epsilon)$, so the map is $(1 + O(\epsilon))$-quasiconformal, as required. Mapping back to the disk by τ^{-1} gives the desired map on D_j. Doing this for each $j = 1, \ldots, n$ proves the lemma. □

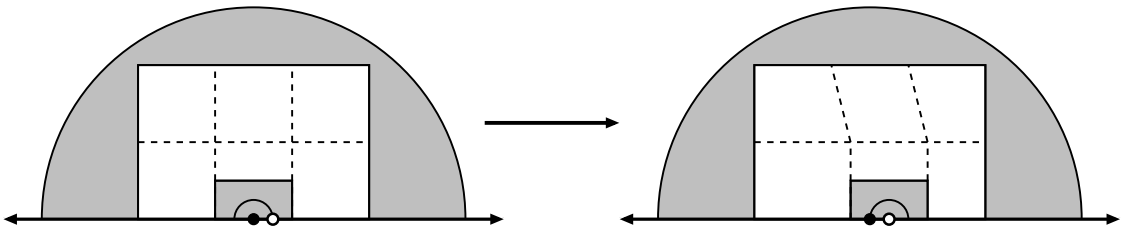

FIGURE 16. Defining a map that moves the origin 0 to a point x. The circular arcs have radii d and ϵd respectively. The map is the identity in the outer shaded region and is a translation in the inner shaded region. In each white rectangle it is an affine stretch or skew map. All the angles in the image quadrilaterals are within $O(\epsilon)$ of 90°, so these affine maps are $O(\epsilon)$-quasiconformal.

Now back to the proof of Lemma 5.1. Let $F : P' \to P$ be the composition of the conformal map from P' to $\mathbb{D}$, followed by Φ, followed by the conformal map of $\mathbb{D}$ to P. This is a quasiconformal map from P' to P with dilatation bounded by $O(\epsilon)$ and mapping each vertex of P' to a vertex of P with equal angle. The push-forward of an equilateral triangulation on P' will be a $(60° + O(\epsilon))$-triangulation of P, away from the vertices. All that remains is to adjust this triangulation to make it equilateral in a neighborhood of each vertex of P.

Suppose $v = v' = 0$ are corresponding vertices in P and P', both with angle $\theta = k \cdot 60°$. Set $\alpha = 3/k$. Then $z \to z^\alpha$ maps the angle θ to 180°, so $G(z) = (F(z^{1/\alpha}))^\alpha$ maps a half-disk centered at the origin conformally to a region also bounded partly by a segment through the orgin. By the Schwarz reflection principle, G extends conformally to a disk around the origin, and hence setting $w = z^{1/\alpha}$, we have $F(w) = G(w^\alpha)^{1/\alpha}$. This implies $F(w) = cw + O(w^2)$ near the origin, for some $c \neq 0$.

Let R be the surface with boundary P. Now take $r > 0$ very small and consider $R \cap D(0, r)$. This corresponds in the plane to a finite sector that equals the intersection of some infinite sector Ω_1 with $D(0, r)$. Define $\Omega_2 = \Omega \setminus D(0, r/3)$. After rescaling, Ω_1 and Ω_2 are compatible in the sense of Lemma 4.4 so we can apply that lemma with f_1 being the identity and $f_2 = F$, as above. If r is small enough, then $|f_1 - f_2| \leq O(r^2) \leq \epsilon r$, so we can apply Lemma 4.4 to define a $1 + O(\epsilon)$ map that interpolates between the identity near 0 and F outside $D(0, 3r)$.

Doing this for every vertex pair in P' and P defines a $1 + O(\epsilon)$-quasiconformal map from P' to P that is complex linear in a neighborhood of each vertex. Thus the image of an equilateral triangulation of P' is a $60^\circ + O(\epsilon)$ triangulation of P that is equilateral in a neighborhood of each vertex, as desired. □

We will need the estimate from the final part of the argument again later, so we record it as a lemma.

Lemma 5.3. *Suppose $0 < \theta \leq 360^\circ$ and that Ω_1 and Ω_2 are Jordan domains such that $\Omega_1 \cap D(0, 1) = \Omega_2 \cap D(0, 1) = S(\theta) \cap D(0, 1)$ and $f : \Omega_1 \to \Omega_2$ is a conformal map such that $f(0) = 0$. Then $f(z) = cz + O(z^2)$ on $D(0, 1/2)$ for some $c \neq 0$.*

6. Triangulations of infinite sectors

As before, $S(\theta)$ denotes the infinite sector of angle θ with positive real half-line as its axis of symmetry. Note that $S(60^\circ)$ comes with a natural equilateral triangulation $\mathcal{G}$ as shown in Figure 17. This triangulation can obviously be extended to a triangulation of the right half-plane, and in this section, we record a computation that gives angle bounds for images of this triangulation under conformal maps of the form $z \to z^\alpha$. See Figure 18 for two examples.

Lemma 6.1. *Consider the grid $\mathcal{G}$ of unit equilateral triangles in $S(60^\circ)$. Let $0 < \alpha \leq 2$. Suppose $T = \Delta ABC \in \mathcal{G}$ and $f^*(T) = \Delta f(A)f(B)f(C)$, where f is a branch of z^α defined on T. Then the interior angles of $f^*(T)$ differ from the corresponding angles of T by at most $|\alpha - 1| \cdot \theta$ where θ is the angle subtended by T from the origin.*

Proof. Consider the angle $\angle f(A)f(B)f(C)$, i.e., the angle between the segments $\overline{f(A)f(B)}$ and $\overline{f(C)f(B)}$. By Rolle's theorem

$$\arg[f(B) - f(A)] = \arg[B - A] + t \arg f'(z),$$

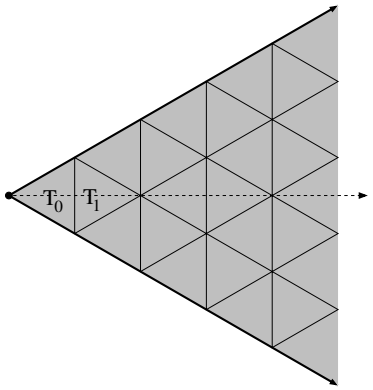

FIGURE 17. The sector $S(60°)$ and its equilateral triangulation $\mathcal{G}$. The triangle containing the vertex of the sector is denoted T_0; the unique triangle adjacent to T_0 is denoted T_1.

for some $z \in \overline{AB}$. Thus the change in angle $|\angle ABC - \angle f(A)f(B)f(C)|$ is at most $|\arg(f'(z)) - \arg(f'(w))|$ where z, w are on $\overline{AB}$ and $\overline{CB}$ respectively. Since $\arg f'(z) = (\alpha - 1)\arg(z)$, the difference $|\arg(f'(z)) - \arg(f'(w))|$ for $z, w \in T$ is no bigger than $|\alpha - 1|$ times the angle subtended by T. □

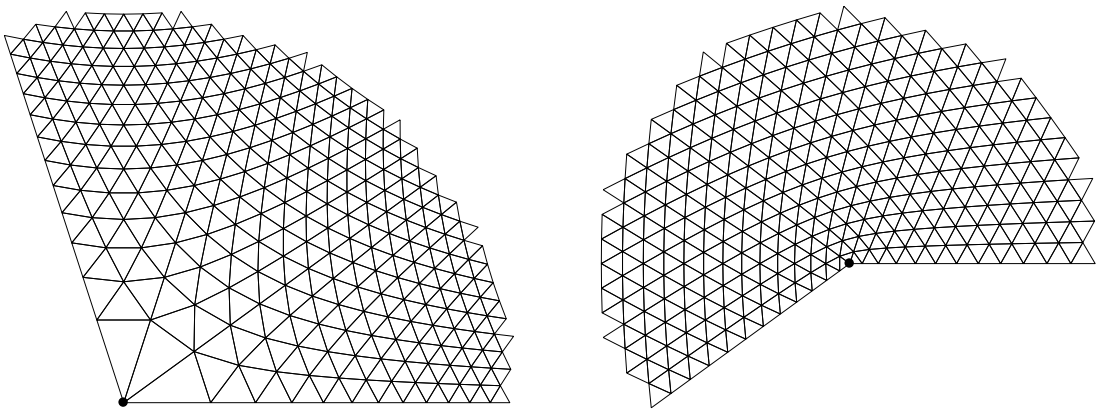

FIGURE 18. Image of the equilateral grid in the upper halfplane under the maps $z^{3/5}$ and $z^{6/5}$. These are the extreme values that keep images of 60° angles between 36° and 72°.

Corollary 6.2. *Suppose $0 < \phi < 90°$. The sector $S(\phi)$ has a triangulation with all angles in $[180° - 2\phi, \phi]$ if $\phi \geq 60°$, and in $[\phi, 90° - \phi/2]$ if $\phi < 60°$. The triangulation is the image of an equilateral triangulation of $S(60°)$ under a power map.*

Proof. First suppose $\phi \geq 60^\circ$ and set $\alpha = \phi/60^\circ$. Consider the image of the triangular grid $\mathcal{G}$, defined above, under the power map $f(z) = z^\alpha$. Note that $\alpha > 1$ and hence $|\alpha - 1| = \alpha - 1$. Let $T_0 \in \mathcal{G}$ be the triangle containing the origin, and let T_1 be the unique triangle in $\mathcal{G}$ that shares an edge with T_0. All other triangles in $\mathcal{G}$ subtend angle $\leq 30^\circ$, so their angles can increase by at most $(\alpha - 1)30^\circ$, and hence these angles are bounded by

$$60^\circ + (\alpha - 1)30^\circ = 30^\circ + \alpha \cdot 30^\circ = 30^\circ + \frac{\phi}{60^\circ} \cdot 30^\circ = 30^\circ + \phi/2 \leq \phi,$$

since $\phi \geq 60^\circ$. The pushed forward triangle $f^*(T_0)$ is isosceles with vertex angle $\phi = \alpha \cdot \theta$, so its angles are in $[90^\circ - \phi/2, \phi] \subset [180^\circ - 2\phi, \phi]$. T_1 is divided into two right triangles by the real axis (each with angles 30° and 60°) and each sub-triangle subtends angle $\leq 30^\circ$. Apply the previous lemma to these sub-triangles. The 30° angle has image angle ψ bounded above and below by

$$60^\circ - \phi/2 = 30^\circ - (\alpha - 1)30^\circ \leq \psi \leq 30^\circ + (\alpha - 1)30^\circ = \phi/2.$$

Doubling the upper bound gives $2\psi \leq \phi$ as the bound for the angle of $f^*(T_1)$ opposite the common edge with $f^*(T_0)$, as desired. The other two angles are equal by symmetry and bounded above by

$$\frac{1}{2}(180^\circ - 2\psi) = 90^\circ - \psi \leq 30^\circ + \phi/2 \leq \phi,$$

since $30^\circ = \frac{1}{2}60^\circ \leq \phi/2$.

For $\phi < 60^\circ$ we have $|\alpha - 1| = 1 - \alpha$, so the push forward $f^*(T)$ of a general triangle $T \in \mathcal{G} \setminus \{T_0, T_1\}$ has angles bounded by

$$60^\circ + (1 - \alpha)30^\circ = 90^\circ - \phi/2 \leq 180^\circ - 2\phi,$$

as desired. Triangle T_0 works out just as before. We split T_1 in half as above. Since $\alpha < 1$ the argument of $f'(z) = \alpha z^{\alpha - 1}$ becomes more negative as we move away from the real axis along the hypotenuse; thus the hypotenuse maps to a concave down curve γ. By conformality, γ meets the real axis at 30°, and thus the segment connecting its endpoints meets the axis at angle $< 30^\circ$. Therefore the corresponding angle ψ of $f^*(T_1)$ is $< 60^\circ$. By symmetry the angles at the other two vertices of $f^*(T_1)$ are equal and bounded above by

$$\frac{1}{2}(180^\circ - 2\psi) \leq 90^\circ - (30^\circ - (1 - \alpha)30^\circ) = 90^\circ - \phi/2. \qquad \square$$

Note that if $T \in \mathcal{G}$ is at distance d from the origin, then it subtends angle $O(1/d)$ so $f^*(T)$ has angles bounded by $60^\circ + O(1/d)$. Thus the pushed forward triangles converge to equilateral as we move away from the vertex of the sector. The following lemma allows us to modify a triangulation pushed forward by a conformal map between polygons to agree with a sector triangulation, as described above, near each vertex. This will be used to show that the bounds in Theorem 1.1 can be attained, not just approximated.

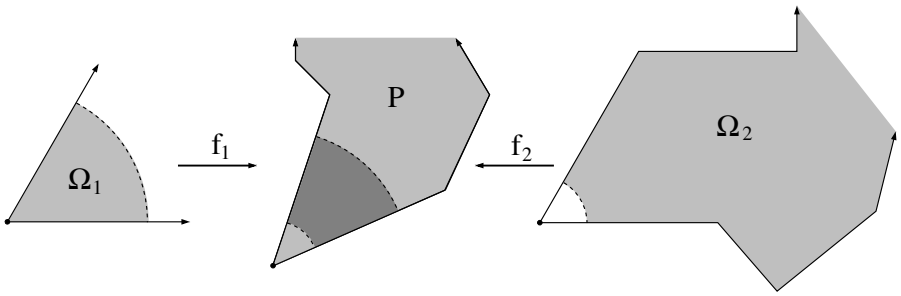

FIGURE 19. Idea for the proof of Lemma 6.3. Near each vertex v of P' we interpolate between the conformal f_2 map from $\Omega_2 \subset P'$ to P (away from v) and a power map f_1 on a sector Ω_1 (near v). The two maps nearly agree on the overlapping region (the image of this overlap is darker in the center picture). This interpolation allows us to attain the sharp angles given by the power map near each vertex; these angles might only be approximated by the conformal map from P' to P.

Lemma 6.3. *Suppose $f : P' \to P$ is a conformal map between polygons that maps vertices to vertices. Suppose $f(v') = v$ where v' is a vertex of P' and v is a vertex of P, with angles $\psi = k \cdot 60^\circ$ and θ respectively. Suppose $\mathcal{T}$ is a nearly equilateral triangulation of P' and $f^*(\mathcal{T})$ the image triangulation of P. If $\mathcal{T}$ is fine enough, then there is a neighborhood U of v and a triangulation $\mathcal{S}$ of P that equals $f^*(\mathcal{T})$ outside U and every triangle of $\mathcal{S}$ touching U has all angles bounded by* $\max(\theta/k, 90^\circ - \theta/2k)$.

Proof. Let Ω' be the interior region of P', and let Ω be the interior region of P. By translating and rotating, we may assume that $v = v' = 0$ and that for sufficiently small $r > 0$ $\Omega' \cap D(v, 3r) = \Omega_1 \cap D(v, 3r)$ where $\Omega_1 = \{z : |\arg(z)| < \psi/2\}$ is an infinite sector of angle θ_v. Define $f_1(z) = z^{\theta/\psi}$; this is a conformal map from Ω_1 to the infinite sector $\Omega_1 = \{z : |\arg(z)| < \theta/2\}$. Define $\Omega_2 = \Omega \setminus D(v, r/3)$ and let f_2 be

f restricted to Ω_2. After rescaling, Ω_1 and Ω_2 are compatible in the sense of Lemma 4.4, and by Lemma 5.3, the conformal maps $f_1^{-1} \circ f_2(x) = cz + O(z^2)$ in $D(0, 3r)$. By replacing f_1 by a constant multiple of itself, we can make $c = 1$ and thus

$$f_2(z) - f_1(z) = f_1(z + O(z^2)) - f_1(z) = O(|z|^2 \cdot |z|^{(\theta/\psi)-1}) = O(|z|^{1+\theta/\psi}).$$

Since $\theta/\psi > 0$, this is less than ϵr if $|z| \le 3r$ is small enough. Therefore Lemma 4.4 applies to (a rescaling of) $\Omega_1, \Omega_2, f_1, f_2$

Thus by taking r sufficiently small, we can apply Lemma 4.4 at each vertex to construct a $(1 + \epsilon)$-quasiconformal map from P' to P that agrees with f outside $U = \Omega' \cap D(v, 3r)$ and that agrees with the power map $Cz^{\psi/\theta}$ inside $D(v, r/3)$ These angles correspond to the triangulation of a sector on angle θ/k given by Corollary 6.2: the image of an equilateral triangulation under a power map. By Corollary 6.2, all these angles are bounded by either θ/k (if $\theta/k \ge 60°$) or by $90° - \theta/2k$ (if $\theta/k < 60°$). Thus the angles are always less than the maximum of these two bounds, as desired. In the intermediate region, $\Omega' \cap (D(v, 3r) \setminus D(v, r/3))$, the triangulation of P' is as close to equilateral as we wish, so the image under the quasiconformal interpolation in this region may be taken as close to equilateral as we wish. This finishes the proof, since the desired angle bound in the lemma is strictly greater than 60°. □

7. The 120°-trick

In this section, we provide the details of the "120°-trick" for triangulating the upper half-plane in a way that uses maximum angle 72°, and near infinity looks like the push forward under $z^{3/2}$ of the standard equilateral mesh of a 120°-sector. This involves cutting a slit in P, as discussed in Sections 1 and 2.

Consider the region Ω shown on the left in Figure 11. This is a 120°-sector with an equilateral triangle at the origin removed. We translate the picture so the 300°-vertex is at the orgin; see the white dot in Figure 20. If we then apply a branch of $z^{6/5}$, the 300° angle becomes 360°, and the two finite segments I, J in $\partial\Omega$ adjacent to it become identified with a radial slit in the image. The two infinite rays in $\partial\Omega$ map to the boundary curve of am infinite Jordan domain Ω'. See lower left in Figure 20. By the Riemann mapping theorem, Ω' can be mapped to the upper half-plane, and the slit maps to a curved arc, meeting the real line at angle 60° (the slit looks quite straight since the tangents at the two endpoints differ by only $\approx 2.75°$).

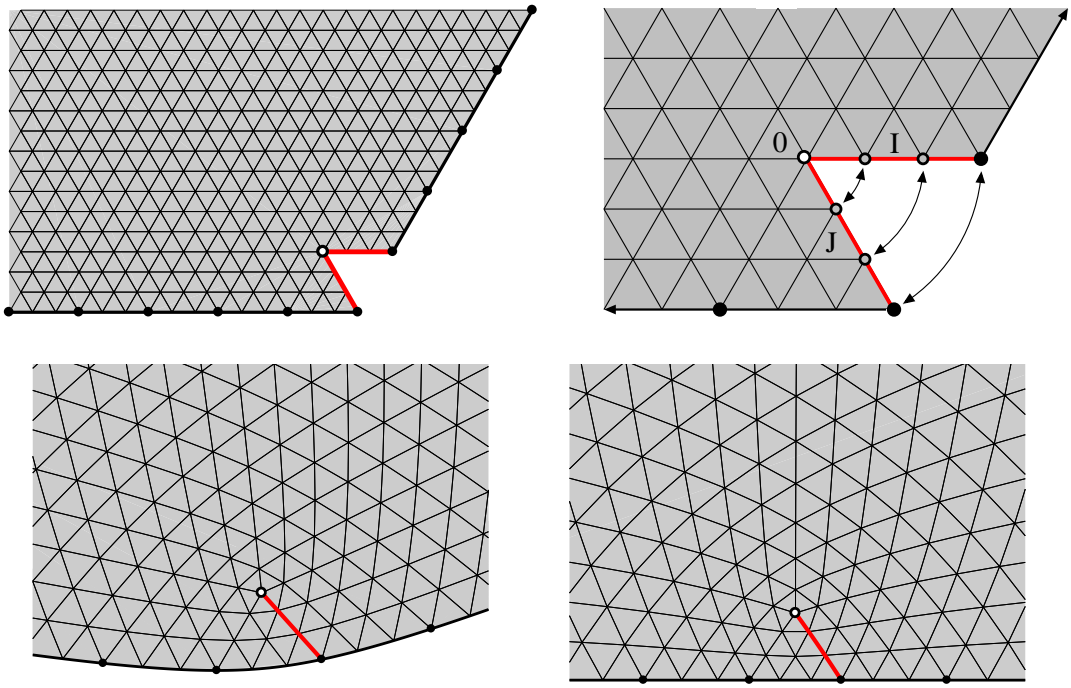

FIGURE 20. The cut 120-sector (top) is mapped to a simply connected region (lower left) by a branch of $z^{6/5}$. This is then mapped to the upper half-plane by a conformal map. Because the power map identifies points on I and J that are equidistant from 0, the push forward of the triangulation is still a triangulation; this is crucial.

Since the power map identifies points on the two segments I, J adjacent to 0 that are equidistant from 0, any equilateral triangulation of Ω will push forward to triangulation of the upper half-plane. If the triangulation is fine enough, then all the pushed forward triangles will be nearly equilateral, except near the corners and tip of the slit. However, near the point v where the slit joins the real line, P looks like the union of a small 60°-sector and a 120°-sector and the map to P' sends each of these to subdomains of P' that contain and are contained in small sectors of the same angles. Thus by Lemma 5.3, the conformal map restricted to each finite sector is approximately linear and the image of the equilateral triangulation of P' is close to equilateral in P near v. This leaves only the tip of slit. In a small neighborhood of the tip, angles are bounded above by $72^\circ + \epsilon$ if the mesh is fine enough, but might

exceed 72°. However, we can replace the mesh in a neighborhood of the tip by the standard mesh of a 360°-sector using Lemma 4.5. This gives the 72° bound.

Lemma 7.1. *Suppose $f : P' \to P$ is a conformal map between polygons that maps vertices to vertices. Suppose $f(v') = v$ where v' is a vertex of P' and v is a vertex of P, with angles* 120° *and* 180° *respectively. Suppose $\mathcal{T}$ is a nearly equilateral triangulation of P' and $f^*(\mathcal{T})$ the image triangulation. If $\mathcal{T}$ is fine enough, then there is a neighborhood U of v and a triangulation $\mathcal{S}$ of P that equals $f^*(\mathcal{T})$ outside U and every triangle of $\mathcal{S}$ touching U has all angles $\leq 72°$.*

Proof. The proof is the same as for Lemma 6.3, except that now we use the mesh coming from the 120°-trick. See Figure 21. □

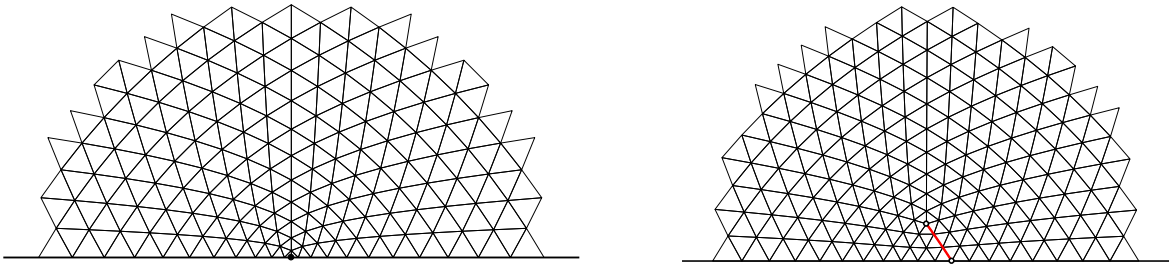

FIGURE 21. The left shows the equilateral triangulation of a 120°-sector pushed forward to the half-plane by $z^{3/2}$. The right shows the triangulation coming from the "120°-trick". These two meshes can be merged using quasiconformal interpolation as described in the text.

8. The 420°-trick

There are two things we can do to increase the ψ-sum for P' by 60° with respect to the θ-sum for P. The first is to introduce a 180°-vertex v in an edge of P and add a corresponding 240°-vertex v' to P'. This clearly increases the ψ-sum by an extra 60° relative to the θ-sum. The angle at v' is subdivided into four equilateral triangles by the nearly equilateral triangulation, and each of these are mapped to four angles of size 45° at v. The opposite angles in the image triangles are $67.5° < 72°$, so this construction will be enough for proving Case 1 of Theorem 1.1.

However, in order to handle Case 2 of Theorem 1.1 we need another "trick" that can add 60° to the ψ-sum relative to the θ-sum, but introduces triangulation angles

no larger than $\frac{5}{7} \cdot 90^\circ \approx 64.2857^\circ$. This is precisely the angle bound we get if a 420°-vertex $v' \in P'$ is mapped to a 360°-vertex $v \in P$. The 360° vertex v can occur as the end vertex of a slit in P, but how do we get a 420°-vertex in P'? We do this by considering a non-planar Riemann surface.

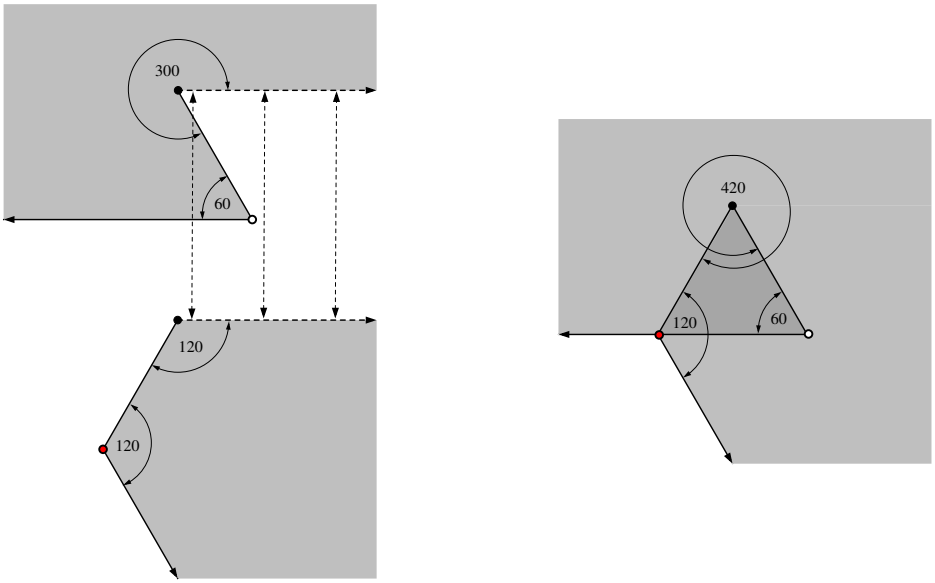

FIGURE 22. Here a 180° vertex in P corresponds to a 420° in P'. This is obtained by making P' a Riemann surface instead of a planar domain. The surface can be constructed from two planar domains glued along the dashed edges of each as illustrated on the left. The darker triangle indicates where the surface has two sheets over the plane.

The idea is illustrated in Figure 22. Consider the two planar regions shown on the left side of the figure and define a Riemann surface by identifying them along the dashed ray. This creates a simply connected Riemann surface R with single boundary curve that is the union of two infinite rays, two finite segments and has three corners of 60°, 420° and 120°.

We can conformally map R to a slit upper half-plane in two steps as illustrated in Figure 23 so that the two segments of ∂R that are adjacent to the 420° angle are identified with the slit, and length measure on these segments is pushed forward to the same measure on the slit. Translate the 420°-vertex to the origin and apply a branch of $z^{6/7}$ defined on R. This maps R to a simply connected planar domain Ω with a straight slit; the two segments of ∂R are identified with this slit in the

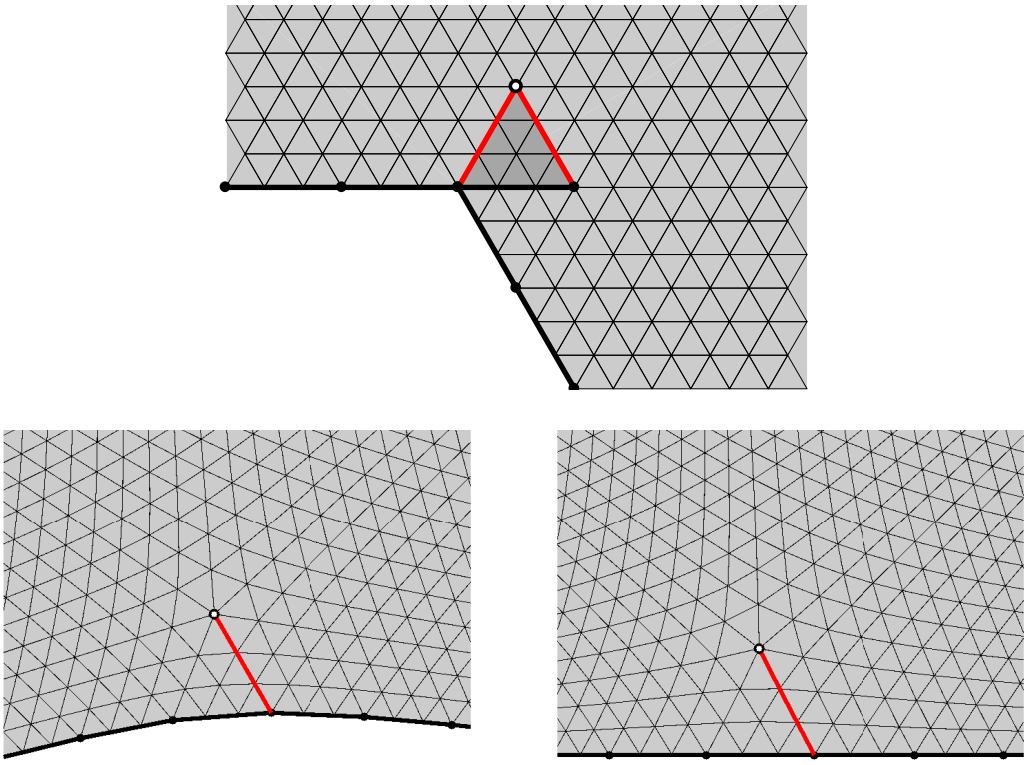

FIGURE 23. The Riemann surface R can be conformally mapped to a slit domain Ω by a branch of $re^{i\theta} \to re^{i6\theta/7}$. This map is followed by a conformal map to the upper half-plane that bends the the straight slit to an analytic arc. (It looks quite straight; the tangent directions only change by about 1° along the arc).

correct way, and the two infinite rays are mapped to disjoint, unbounded arcs on $\partial\Omega$. The domain Ω can then be conformally mapped to a half-plane. Thus equilateral triangulations of R will be mapped to triangulations of the upper half-plane.

9. Necessity in Theorem 1.1

Proof. For completeness, we include the details of the proof of necessity that was sketched preceding the statement of Theorem 1.1. We also restate our conditions in the notation used by Gerver in [33], who also proved the necessity of these conditions.

Fix $60^\circ < \phi < 90^\circ$ and suppose $\mathcal{T}$ is a ϕ-triangulation of P. Let V_P be the vertex set of P and $|V_P|$ the number of points in V_P (in general we let $|X|$ denote the number of elements in a set X). As before, for $v \in V_P$, let $L(v)$ denote the number of triangles

containing v. Let F (for faces) be the number of triangles in $\mathcal{T}$, and E the number of edges. Let $V_{\mathcal{T}}$ be the vertices of the triangulation $\mathcal{T}$. If an interior angle θ of P is subdivided into k sub-angles all in $I(\phi)$, then $\theta \in k \cdot I(\phi)$. Thus a ϕ-triangulation of P gives an admissible labeling of V_P. This is necessity in Case 1.

Let $V_{\mathcal{T}}(k) = \{v \in V_{\mathcal{T}} : L(v) = k\}$, i.e., the vertices that are in k triangles. Set

- $r_k = |V_{\mathcal{T}}(k) \cap V_P|$ (vertices of P in k triangles),
- $q_k = |V_{\mathcal{T}}(k) \setminus P|$ (interior vertices of $\mathcal{T}$ in k triangles),
- $s_k = |V_{\mathcal{T}}(k) \cap (P \setminus V_P)|$ (boundary vertices of $\mathcal{T}$ that are not vertices of P).

With this notation, $|V_P| = \sum_k r_k$, $|\mathrm{int}(\mathcal{T})| = \sum_k q_k$, and $|\partial\mathcal{T}| = \sum_k s_k + \sum_k r_k$. Given a labeling $L : V_P \to \mathbb{N}$ as above, we have $\sum_k kr_k = \sum_{v \in V_P} L(v)$ and hence

$$\sum_k (3-k) r_k = 3|V_P| - \sum_v L(v) = 6 - \kappa(L).$$

Therefore $\kappa(L) \le 0$ if and only if $\sum_k (3-k) r_k \ge 6$, and equality holds simultaneously. This is the notation used by Gerver in [33].

We have the relations

- $F - E + |V_{\mathcal{T}}| = 1$ (Euler's formula),
- $|V_{\mathcal{T}}| = \sum_k q_k + \sum_k r_k + \sum_k s_k$ (every vertex is in V_P, $P \setminus V_P$ or $V_{\mathcal{T}} \setminus P$),
- $3F = \sum_k kq_k + \sum_k kr_k + \sum_k ks_k$ (triangle corners counted in two ways),
- $2E = 3F + \sum_k r_k + \sum_k s_k$ (triangles sides counted in two ways),

Combining these four equations and eliminating F, $|V_P|$, E and $|V_{\mathcal{T}}|$ we get

$$\sum_k (6-k) q_k + \sum_k (3-k) r_k + \sum_k (3-k) s_k = 6, \tag{9.1}$$

in Gerver's notation, or equivalently using discrete curvatures:

$$\sum_{v \in \mathrm{int}(\mathcal{T})} \kappa(v) + \sum_{v \in V_P} \kappa(v) + \sum_{v \in \partial\mathcal{T} \setminus V_P} \kappa(v) = 6. \tag{9.2}$$

This is the discrete Gauss-Bonnet formula, (1.1). For acute triangulations we have $s_1 = s_2 = 0$, and hence the third term in (9.1) and (9.2) is non-positive, i.e., $\sum_{v \in \mathrm{int}(\mathcal{T})} \kappa(v) + \sum_{v \in V_P} \kappa(v) \ge 6$.

In Case 2 of Theorem 1.1, $\phi < 72°$, so every interior vertex has degree ≥ 6. This implies $q_1 = \cdots = q_5 = 0$ and thus the first term in (9.2) is also non-positive, i.e., $\kappa(L) = 6 - \sum_{v \in V_P} \kappa(v) \le 0$, as desired.

In Case 3, $60^\circ < \phi < \frac{5}{7}90^\circ$, so every interior vertex of $\mathcal{T}$ has degree six and every vertex in $\partial\mathcal{T} \setminus V_P$ has degree three. Thus $\sum_{v\in\text{int}(\mathcal{T})} \kappa(v) = \sum_{\partial\mathcal{T}\setminus V_P} \kappa(v) = 0$ and so (9.2) implies $\kappa(L) = 0$, as desired. □

10. Sufficiency in Theorem 1.1: Case 1

Proof. We want to show that any polygon P (possibly after adding extra vertices) can be conformally mapped to a 60°-polygon P', with the restrictions on the angles given by Table 1. We will use the 120°-trick to "fix" the pushed forward triangulation in a neighborhood of a few boundary points, but the 420°-trick is not needed until the proof of Cases 2 and 3 in the next section.

The Schwarz-Christoffel formula gives a conformal map f of the disk onto a polygonal region P in terms of two types of data. First are the angles of P: suppose $V_P = \{v_j\}_1^N$ are the vertices of P and the interior angle at v_j is $\alpha_j \cdot 180^\circ$. Second, suppose f maps $z_j \in \mathbb{T}$ to $v_j \in P$; these points are called the prevertices or Schwarz-Christoffel parameters of f. Then the conformal map f is given by

$$f(z) = A + C \int^z \prod_{j=1}^{N} (1 - \frac{w}{z_j})^{\alpha_j - 1} dw, \tag{10.1}$$

for some appropriate choice of constants A, C. See e.g., [25], [50], [58]. The formula was discovered independently by Christoffel in 1867 [22] and Schwarz in 1869 [55], [54]. For other references and a brief history, see Section 1.2 of [25]. Given a polygon P, the angles are known, but the prevertices must be solved for.

Given N distinct points $\mathbf{z} = \{z_1, \ldots, z_N\}$ on the unit circle and N real values $\{\alpha_1, \ldots, \alpha_N\}$ summing to $N - 2$, Formula (10.1) defines a locally 1-1 holomorphic function on the disk that maps each component of $\mathbb{T} \setminus \mathbf{z}$ to line segment, with the segments meeting at $f(z_k)$ making interior angle $\alpha_k \cdot 180^\circ$. The map given by (10.1) is always locally 1-1 on $\mathbb{D}$, but need not be globally 1-1 in general. In this case, the image is a Riemann surface with an obvious projection onto the plane. For the proof of Case 1 of Theorem 1.1 we can arrange for the image to be a planar 60°-polygon, although in the proof of Cases 2 and 3, given in the next section, the image may be a non-planar 60°-surface (this occurs when we apply the 420° trick).

Given an N-gon P, we take some conformal map f of its interior to the unit disk, $\mathbb{D}$. The N vertices of P map to N distinct points $\mathbf{z} = \{z_1, \ldots, z_N\}$ on the unit circle

$\mathbb{T}$. We then want to choose N real values $\psi_k \in Z = \{60°, 120°, 180°, 240°, 300°\}$ so that $\sum_k \psi_k = 180(N-2)$. If this is possible, we then set $\alpha_k = \psi_k/180$ and apply the Schwarz-Christoffel formula to get a map $g : \mathbb{D} \to P'$. Then $g \circ f : P \to P'$ is the desired map. However, as noted in Sections 1 and 2, such a choice of angles ψ_k may not be possible without adding extra vertices to P.

First choose six interior points of some edge of P. We call these the "extra" vertices of P. This creates an M-gon with $M = N + 6$. These are 180°-vertices in P and are assigned to have angle $\psi_v = 120°$ in P'. Assign angle 180° to every other vertex of P', so the ψ-angle sum is $6 \cdot 120° + 180°N = (M-2)180°$. Applying Schwarz-Christoffel gives a a 60°-hexagon, as in Figure 24.

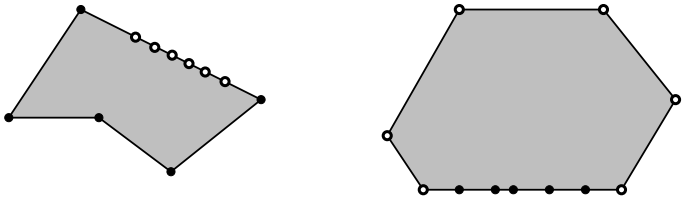

FIGURE 24. In the proof of Case 1 of Theorem 1.1 we can assume P' is planar. The first step is to choose six "extra" vertices on one edge of P and make these correspond to six 120°-vertices in P'.

Next we modify the angle assignments to get a P' that approximates this hexagon. Let $L : V_P \to \mathbb{N}$ be a ϕ-admissible labeling of the vertices of P. For $v \in V_P$, assign angle $\psi_v = 60° \cdot L(v)$ to the corresponding vertex v' of P'. In order to adjust the angle sums, for each vertex v of P we define either 0, 1 or 2 "associated vertices". The new vertices will be in the edge of P that begins with v (P has the counterclockwise orientation with the domain interior on the left) and may be taken as close to v as we wish. The vertices associated to v on P have angle 180° and the corresponding vertices associated to v' in P' have angle either 120° or 240°. The following rules for making the assignments are illustrated in Figure 25. Suppose v is an original vertex of P with interior angle θ_v:

(i) if $0 < \theta_v \le 72°$, set $\psi_v = 60°$ and add two vertices each with angle 240°,
(ii) if $72° < \theta_v \le 144°$, set $\psi_v = 120°$ and add one vertex with angle 240°,
(iii) if $144° < \theta_v \le 216°$, set $\psi_v = 180°$ and add no associated vertices,
(iv) if $216° < \theta_v \le 288°$, set $\psi_v = 240°$ and add one vertex with angle 120°,

(v) if $288^\circ < \theta_v \leq 360^\circ$, set $\psi_v = 300^\circ$ and add two vertices of angle 120°.

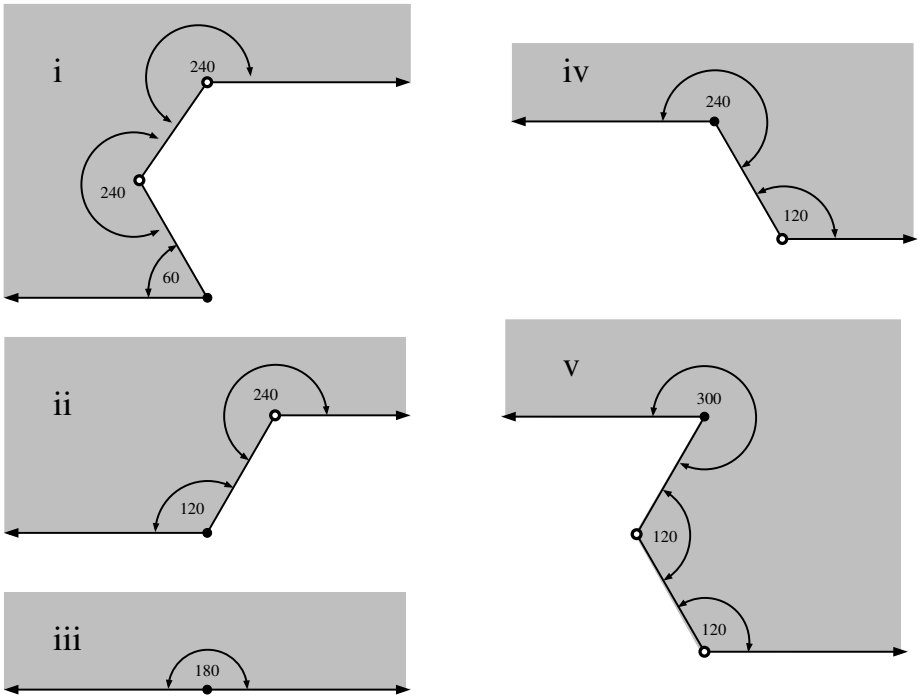

FIGURE 25. The five cases for assigning image angles and associated vertices. In each case the black indicates the image $v' \in P'$ of a vertex $v \in P$ and the white dots the new associated vertices; each of the latter corresponds to a a 180° vertex in P.

The angles at the extra vertices associated to v were chosen precisely so the curve entering v is parallel to the curve leaving last vertex associated to v. Thus if the distance between v and its associated vertices is very small, the entering and exiting segments will be parallel, and they will have very small perpendicular displacement, i.e., they will look like a single line segment. See Figure 26. Thus if every vertex is sufficiently close to its associated vertices, the minimal sub-arc of P' containing all the vertices, except for the six extra vertices, is as close as we wish to a line segment in the Hausdorff metric. In particular, P' is not self-intersecting and so is a planar 60°-polygon. By Lemma 5.1, P' has nearly equilateral triangulations. In the remainder of the proof we will take this triangulation as fine as is needed (but only finitely many conditions are involved, so we finish with a positive grid size).

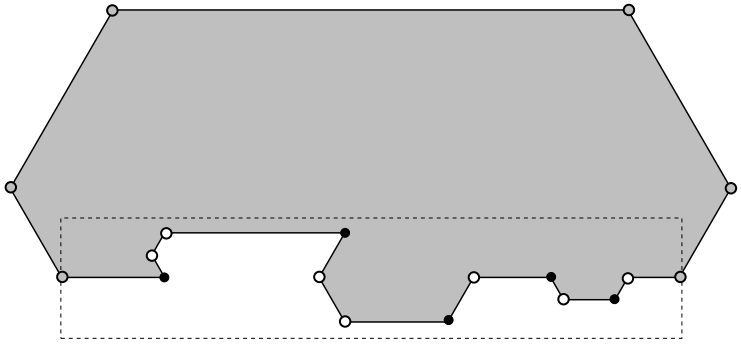

FIGURE 26. The 60°-polygon P'. The six gray points are the "extra" vertices added at the beginning, the black points are the images of the original vertices, and the white points are the associated vertices. If each black vertex is very close to its associated white vertices, then the arc inside the dashed box mostly (in terms of length) consists of horizontal segments, and will approximate a horizontal segment.

Each original vertex with angle $\theta_v \geq 36°$ was assigned an image angle ψ_v in the allowable range from Table 1. Thus transferring a nearly equilateral triangulation of P' gives a triangulation of P with all angles between 36° and 72° except possibly in small neighborhoods of these vertices, where all the angles are between $36° - \epsilon$ and $72° + \epsilon$, and ϵ can be made as small as we wish be taking the triangulation fine enough. In a neighborhood of each such vertex, we may use Lemma 6.3 to merge the pushed forward triangulation with a sector triangulation with angle bounds $36°, 72°$.

For each original vertex with interior angle $\theta_v < 36°$ the same argument applies, except that now we get the bounds in the interval $I(\theta_v) = [\theta_v, 90° - \theta_v/2]$. Again, we may use interpolation to locally merge the pulled back triangulation (which might only approach the desired bounds as the triangulation gets finer), with a sector triangulation satisfying the precise desired bounds.

Next, consider the associated vertices with angles $> 120°$; Cases (i) and (ii) above. In Case (i) each 240°-vertex is hit by 4 equilateral triangles and so each 60° sub-angle is mapped to an angle of size $180°/4 = 45°$. In this case, the interpolation with a sector triangulation isn't needed; with small enough distortion, the angles are already inside $[36°, 72°]$. Case (ii) is the same, except there is only one associated vertex.

There are no associated vertices in Case (iii).

Finally, we consider Cases (iv) and (v). Here we only use image angles of size $120°$. Such an angle is divided into two $60°$ angles that are mapped to $90°$ by the conformal map. These angles are too large, so we use Lemma 7.1 to interpolate between the conformal image triangulation and the triangulation of the half-plane coming from the $120°$-trick. This gives a triangulation of with angles in $I(36°) = [36°, 72°]$ in a neighborhood of each associated vertex. This completes Case 1 of Theorem 1.1. □

Proof of Corollary 1.3. If $\phi \geq 72°$, then (see Figure 8)

$$\bigcup_{k\geq 1} k \cdot I(\phi) = [180° - 2\phi, \infty).$$

So for $\phi \in [72°, 90°)$ having a ϕ-admissible labeling the same as $\phi \geq 180° - 2\theta_{\min}$. Therefore P must have a ϕ-triangulation for

$$\phi = \max(72°, 90° - 2\theta_{\min}) = 90° - \min(36°, \theta_{\min})/2.$$

Thus the infimum defining $\Phi(P)$ is at most this value, as desired. □

The upper bound in Corollary 1.3 implies every angle in the triangulation is at least $\min(\theta_{\min}, 36°)$. However, the proof of Theorem 1.3 actually proves the following, slightly stronger, lower bound: every angle in the triangulation is larger or equal to

$$\max\left(\min(\theta_{\min}, 36°), \min(\theta_{\min}/2, 48°), \min(\theta_{\min}/3, 54°)\right).$$

This formula is somewhat clearer when graphed, as in Figure 27. The first term follows directly from Corollary 1.3. The second term holds because any angle $72° \leq \theta \leq 96°$ can be divided into two angles of size $\theta/2$ and larger angles can be divided into two or more angles $\geq 48°$. Similarly, the third term arises because any angle $144° \leq \theta \leq 162°$ can be divided into three angles of size $\theta/3$ and larger angles can be divided into three or more angles $\geq 54°$.

11. Sufficiency in Theorem 1.1: Cases 2 and 3

Proof. We have already proven sufficiency in Case 1. To prove it in the other two cases, we just have to modify the construction in the proof of Case 1 to avoid using the $120°$-trick in Case 2 (this forces an angle $\geq 72°$), and to avoid both the $120°$-trick and the $420°$-trick in Case 3 (the latter forces angles $\geq \frac{5}{7} \cdot 90°$).

Suppose L is a ϕ-admissible labeling of V_P so that $\kappa(\phi) = \kappa(L)$ (i.e., choose L to minimize $|\kappa(L)|$ among admissible labelings). As before, let θ_v denote the angle of

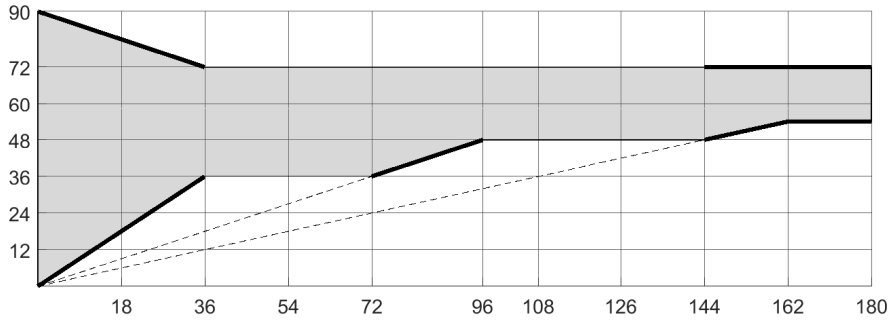

FIGURE 27. If P has minimal angle $0 < \theta_{\min} < 180°$ (plotted on the horizontal axis), then P has a triangulation with all angles inside the interval above $\theta_{\min}$. For example, if $\theta_{\min} = 108°$ the interval is $[48°, 72°]$. Bold lines indicate values that must be attained by any upper-optimal triangulation, e.g., $\theta_{\min} = 80°$ implies $40°$ is attained by any $72°$-triangulation of P.

P at vertex v, and for each vertex v in P, suppose $\psi_v = L(v) \cdot 60°$ is the tentative corresponding angle of v' in P'. As we have noted before,

$$\begin{aligned}\sum_v \theta_v &= (|V_P| - 2)180° = 60°(3|V_P| - 6) \\ &= 60° \left(3|V_P| - 6 - \sum_v L(v) + \sum_v L(v) \right) \\ &= 60° \left(-\kappa(L) + \sum_v L(v) \right) = -60° \cdot \kappa(L) + \sum_v \psi_v.\end{aligned}$$

Thus in Case 2 ($\kappa(L) \leq 0$) we only need to introduce $180°$-vertices on P that correspond to $240°$-vertices in P'. If $\phi \geq 67.5°$, we can do this by replacing the pushed forward triangulation from P' by the $240°$-sector triangulation. If $\frac{5}{7} \cdot 90° \leq \phi < 67.5°$ then we replace it with the triangulation of the half-plane obtained by the $420°$-trick. This proves sufficiency in Case 2.

Finally, if $\kappa(L) = 0$, then no extra vertices or "tricks" are needed. We simply use a fine enough triangulation pushed forward by the conformal map from P' to P and replace it in a neighborhood of each vertex by the appropriate sector mesh. □

Proof of Corollary 1.17. By construction, all the interior vertices of our triangulation have degree 6, except for the single degree 7 vertex used in each application of the "420°-trick" and the vertex of degree 5 used in the "120°-trick". The first is only

used in Case 2 of Theorem 1.1 and is only needed for angles $< 67.5°$, since using a $240°$ sector mesh will work for larger angles. The number of times we need to apply the $420°$-trick is $(\sum_P \theta_v - \sum_{P'} \psi_v)/60° = -\kappa(\phi)$, so this is the number of degree 7 vertices.

One degree 5 vertex is created in each application of the $120°$-trick. This occurs only in Case 1 and only if $\sum_P \theta_v < \sum_{P'} \psi_v$; otherwise we can use $240°$-vertices in P' to make up the gap. Thus only $\max(0, \kappa(\phi))$ degree 5 vertices need to be created. □

Proof of Corollary 1.4. In [33], Gerver proved the conditions in Theorem 1.1 are implied by the weaker condition that for every $\epsilon > 0$, the polygon P has a $(\phi + \epsilon)$-dissection. This and Theorem 1.1 show that (1) ⇒ (3). Since (3) ⇒ (2) ⇒ (1) is trivial, the corollary is proven. □

To recreate Gerver's argument in [33], redefine q_k to be the number of interior vertices of the triangulation that are shared with k triangles and are not interior to any edges of the triangulation. Also, redefine s_k to be the number of vertices of the triangulation that are shared by k triangles and that lie on the interior of an edge of P or of an edge of some triangle. The argument in the second half of Section 10 now proceeds as before, showing that having a $(\phi + \epsilon)$-dissection for every $\epsilon > 0$ implies the conditions in Theorem 1.1 must hold.

12. Some examples

Proof of Corollary 1.7. We compute the optimum upper bound Φ_N for triangulating the regular N-gon. The cases $N = 3$ and $N = 6$ are trivial; these have equilateral triangulations, so $\Phi_3 = \Phi_6 = 60°$. Otherwise, there are N interior angles of size $\theta_N = 180° - 360°/N \geq 90°$. Since these are all $> 36°$, Corollary 1.3 says $\Phi_N \leq 72°$, so we only have to check whether an even smaller bound is possible.

For $N \geq 10$, the interior angles are $\geq 144°$, and hence the ϕ-admissible labels for $\phi < 72°$ are at least 3. Then any ϕ-admissible label satisfies $\kappa(L) \geq 6 > 0$, so we must be in Case 1, so $\Phi_N = 72°$. (This case also follows from Corollary 1.10).

For $N = 9$, the interior angle is $\theta_9 = 140°$. If $\phi < 70°$ then $\theta_9 \notin 2 \cdot I(\phi)$, so all the ϕ-admissible labels are ≥ 3, which implies $\kappa(L) \geq 6$; thus such ϕ's don't work. However, for $\phi = 70°$ we can take six labels equal to 2 and three equal to 3; this

labeling satisfies $\kappa(L) = 6 - 6(3-2) - 3(3-3) = 0$. Thus Case 2 holds for $\Phi_9 = 70^\circ$ and this must be the sharp upper bound.

For $N = 8$, the same argument holds by considering $\theta_8 = 135^\circ$ and $\phi = 67.5^\circ$. Below this value, admissible labels have positive curvature, but for this value we obtain a zero curvature label by taking six labels 2 and two of 3. Thus $\Phi_8 = 67.5^\circ$.

For $N = 7$, we have $\theta_7 = \frac{5}{7} \cdot 180^\circ \approx 128.5714$, and apply the argument to $\Phi_7 = \frac{5}{7} \cdot 90^\circ \approx 64.2857$. The only Φ_7-admissible label for θ_7 is 2, and the curvature of this labeling is $6 - 7(3-2) = -1$. Therefore there is a Φ_7-triangulation, and this is sharp since there are no zero curvature labelings for smaller ϕ's.

For $N = 4$ the internal angles are 90° so the only ϕ-admissible labels for $\phi \leq 72^\circ$ are ≥ 2, and hence any such ϕ-admissible label L satisfies $\kappa(L) \geq 6 - 4 \cdot (3-2) = 2 > 0$. Thus Cases 2 and 3 of Theorem 1.1 can't hold and we must be in Case 1, i.e., $\Phi_4 \geq 72^\circ$. By our remark at the beginning of the proof, we must have equality. Exactly the same argument works for $N = 5$, but using $\kappa(L) \geq 6 - 5 \cdot (3-2) = 1 > 0$. □

Proof of Corollary 1.8. By Corollary 1.3, $\phi(P) \leq 72^\circ$. The polygon P only has angles of 90°, 180° or 270°, so suppose P has n_{90}, n_{180} and n_{270} angles of each size. Then $|V_P| = n_{90} + n_{180} + n_{270}$ and the angle sum formula for polygons implies $n_{270} = n_{90} - 4$. Thus $2n_{270} = |V_P| - 4 - n_{180}$. Any ϕ-admissible labeling for $\phi < 90^\circ$ gives the 90°-vertices label 2, the 180°-vertices labels ≥ 3 and the 270°-vertices labels ≥ 4. Thus the smallest admissible label sum is

$$2n_{90} + 3n_{180} + 4n_{270} = 2n_{90} + 3n_{180} + |V_p| - 4 - n_{180} + 2n_{270} = 3|V_P| - 4,$$

so $\kappa(L) \geq 2$ for any $\phi < 90^\circ$ and any ϕ-admissible labeling L. Thus we must be in Case 1 and 72° is the sharp angle bound. Moreover, there is a 72°-admissible labeling (the minimal one) with $\kappa(L) = 2$, so we can apply the 120°-trick twice and construct a triangulation with exactly two vertices of degree 5 (the rest are degree 6). □

The proof above still holds if the angles are perturbed slightly (the bounds on the labels don't change), so the axis-parallel N-gons are in the interior of the set of all N-gons with sharp bound 72°, e.g., Corollary 1.11. The proof also works if we allow angles of 360°; the analogous arithmetic shows the minimal labeling for any $\phi < 90^\circ$ is still 2. However, in this case the polygon is not simple and the optimal triangulation need not be consistent across "slits" at the 360° vertices.

Proof of Corollary 1.9. If $\theta_{\min} \leq 36^\circ$, the statement is just a special case of Corollary 1.3. So suppose $\theta_{\min} > 36^\circ$. Then again my Corollary 1.3, we have $\Phi(P) \leq 72^\circ$. If $\Phi(P) < 72^\circ$ then by Theorem 1.1 P has a labeling L of non-positive curvature. This means that $6 - \sum_1^3 (3 - L(v)) \leq 0$ or $\sum_1^3 L(v) \leq 3$, which implies $L(v) = 1$ for all three vertices. Thus the optimal triangulation does not subdivide any of the three angles of the triangle, so all these angles occur in the triangulation. Thus $\Phi(T) \geq \theta_{\max}$. Since we can take T as a triangulation of itself, we get equality. □

Proof of Corollary 1.10. If all angles of P are $\geq 144^\circ$, then for any $\phi < 72^\circ$, any ϕ-admissible labeling is at least 3 at every vertex, and hence has curvature ≥ 6. By Corollary 1.3, 72° is therefore the sharp angle bound. If the minimum angle of P is $\geq 162^\circ$, then every angle of P can be split into three or more angles between 54° and 72° and the triangulation only uses interior vertices of degree 5 and 6. Thus all angles in the triangulation can be taken in $[54^\circ, 72^\circ]$. If we also assume that all angles are $\leq 216^\circ$, then taking all labels equal to 3 is 72°-admissible, and has curvature 6, so we need only six applications of the 120°-trick. □

13. Computing $\Phi(P)$ in linear time

Proof of Corollary 1.6. First check whether every angle of P is a multiple of 60°. If so, then $\Phi(P) = 60^\circ$. If not, find the smallest angle $\theta_{\min}$ of P. If $\theta_{\min} \leq 36^\circ$, then $\Phi(P) = 90 - \theta_{\min}/2$ by Corollary 1.3. If $\theta_{\min} \geq 144^\circ$ then $\Phi(P) = 72^\circ$ by Corollary 1.10. All this can be done in time $O(|V_P|)$.

Otherwise we may assume $36^\circ < \theta_{\min} < 144^\circ$, and we claim that computing $\Phi(P)$ reduces to finding one or both of

$$\phi_\infty = \inf\{\phi \in [60^\circ, 90^\circ] : \kappa(\phi) < \infty\},$$

$$\phi_0 = \inf\{\phi \in [60^\circ, 90^\circ] : \kappa(\phi) = 0\}.$$

Since $I(90^\circ) = [0^\circ, 90^\circ]$, 4 is a 90°-admissible label for any vertex of any polygon, so we always have $\kappa(90^\circ) < \infty$. This implies ϕ_∞ is well defined. Computing ϕ_∞ in time $O(|V_P|)$ is easy: for each $v \in V_P$, we find the smallest ϕ so that v has a ϕ-admissible label (time $O(1)$ per angle) and then take the maximum of these $|V_P|$ values.

Increasing an 90°-admissible label gives another 90°-admissible label, so $\mathcal{K}(90°)$ is a half-infinite interval of the form $\{k \geq k_0\}$. Thus $\kappa(90°) \geq 0$ for any polygon. If $\kappa(90°) > 0$, then $\kappa(\phi) > 0$ for all $\phi < 90°$ and hence $\Phi(P) = \max(72°, \phi_\infty)$.

We may henceforth assume that $\kappa(90°) = 0$. Thus ϕ_0 is well defined and $\phi_0 \leq 90°$. If $\kappa(\phi_\infty) = 0$, then $\phi_\infty = \phi_0$ and $\Phi(P) = \phi_\infty$.

So assume $\kappa(\phi_\infty) \neq 0$; thus $\phi_\infty < \phi_0$. We consider the cases $\kappa(\phi_\infty) > 0$ and $\kappa(\phi_\infty) < 0$ separately.

If $\kappa(\phi_\infty) > 0$, then $\kappa(\phi)$ is a decreasing, non-negative function of ϕ and

- if $\phi_\infty \geq 72°$, then $\Phi(P) = \phi_\infty$;
- if $\phi_\infty < 72°$ and $\phi_0 \geq 72°$, then $\Phi(P) = 72°$;
- if $\phi_0 < 72°$, then $\Phi(P) = \phi_0$.

Otherwise, $\kappa(\phi_\infty) < 0$. Then $\kappa(\phi)$ is non-positive and increasing, and we have:

- if $\phi_\infty \geq \frac{5}{7} \cdot 90°$, then $\Phi(P) = \phi_\infty$;
- if $\phi_\infty < \frac{5}{7} \cdot 90°$ and $\phi_0 \geq \frac{5}{7} \cdot 90°$, then $\Phi(P) = \frac{5}{7} \cdot 90°$;
- if $\phi_0 < \frac{5}{7} \cdot 90°$, then $\Phi(P) = \phi_0$.

Compute $\kappa(72°)$. If this is non-zero, then $\phi_0 > 72°$. In every case where this holds (the first two bullets in each triple), $\Phi(P)$ is determined from ϕ_∞ alone.

We have now reduced finding $\Phi(P)$ to computing ϕ_0, assuming that $\kappa(72°) = 0$, and hence that $\phi_0 \leq 72°$. Note that $\kappa(\phi) = \min(\kappa^+(\phi), 0) + \max(\kappa^-(\phi), 0)$, where

$$\kappa^-(\phi) = -3|V_P| + 6 + \sum_v \inf\{k \in \mathbb{N} : \theta_v \in k \cdot I(\phi)\},$$

$$\kappa^+(\phi) = -3|V_P| + 6 + \sum_v \sup\{k \in \mathbb{N} : \theta_v \in k \cdot I(\phi)\},$$

are the smallest and largest elements of $\mathcal{K}(\phi)$. For a single value of ϕ, each of these can be computed in time $O(|V_P|)$, hence so can $\kappa(\phi)$. Moreover, given each angle θ_v of P, we can compute the values of $\phi \in (60°, 72°]$ where θ_v lies on the boundary of one of the triangles in Figure 8. There are 10 possible triangles, so at most 10 possible ϕ's for each θ_v. In fact, Figure 8 shows at most 5 triangles can be hit by a single horizontal line of height $\theta \in [0, 360°]$ over the interval $[60°, 72°]$. This gives a set $X_1 \subset (60°, 72°]$ of size $\leq 5|V_P|$ that contains all possible ϕ values where κ^- and κ^+ can have jumps. If we were to sort X_1, then we could compute these functions at every jump point by summing jumps from left to right, and then find ϕ_0 by searching

for the smallest ϕ value so that $\kappa(\phi) = 0$. This takes time $O(|V_P| \log |V_P|)$ due to the sorting, but ϕ_0 can be computed even faster.

Recall that we are now assuming $\kappa(\phi_\infty) \neq 0$ and $\kappa(72^\circ) = 0$. Find the median value ϕ_1 of X_1; this can be done in time $O(|X_1|)$ by the median-of-medians algorithm in [18]. (See also [2] for some history and updates of this algorithm.) Compute $\kappa(\phi_1)$ in time $O(|X_1|)$. If $\kappa(\phi_1) = 0$, then $\phi_0 \in X_1 \cap [\phi_\infty, \phi_1]$ and otherwise $\phi_0 \in X_1 \cap [\phi_1, 72^\circ]$. In either case, we now know that ϕ_0 is contained in a subinterval X_2 of X_1 with at most $\frac{1}{2}|X_1| + 1$ elements. Thus $|X_2| \leq \frac{3}{4}|X_1|$ if $|X_1| \geq 4$. We can construct X_2 in time $O(|X_1|)$ by comparing each element of X_1 to ϕ_1.

We inductively create intervals $X_1 \supset X_2 \supset X_3 \supset \dots$ containing ϕ_0 (by induction, κ will be non-zero at the leftmost point of X_n and zero at the rightmost point). Given X_n, we find its median ϕ_n in time $O(|X_n|)$ by the median-of-medians algorithm. We can compute $\kappa(\phi_n)$ in time $O(|X_n|)$ because we already know κ at the leftmost endpoint of X_n and we can sum the jumps between this point and ϕ_n by examining each element of X_n. If $\kappa(\phi_n) = 0$ we let X_{n+1} be the elements of X_n that are $\leq \phi_n$, and otherwise the elements of X_n that are $\geq \phi_n$. Clearly X_{n+1} has at most $\frac{1}{2}|X_n|+1 \leq \frac{3}{4}|X_n|$ elements and takes $O(|X_n|)$ work to compute. Stop when $|X_n| \leq 4$, and compute κ at all these values to find ϕ_0. The total time taken is

$$O(|X_1| + |X_2| + \dots) = O(|X_1|)(1 + 3/4 + (3/4)^2 + \dots) = O(|V_P|). \quad \square$$

14. Continuity of Φ

Proof of Corollary 1.11. Suppose P is an N-gon and $\{P_n\}$ is a sequence of N-gons converging to P. This means the ordered list of vertices converges in $\mathbb{R}^{2N}$.

First suppose P has a ϕ-triangulation $\mathcal{T}$. Choose ϵ so small that any two distinct vertices of $\mathcal{T}$ are at least distance ϵ apart. For any $\delta > 0$ choose n so large that all the interior vertices of $\mathcal{T}$ are contained inside P_n, and each boundary vertex of $\mathcal{T}$ is within $\delta \cdot \epsilon$ of a point on P_n. Move the boundary points of $\mathcal{T}$ to these points on P_n. This creates a triangulation of P_n whose angles are within $O(\delta)$ of the corresponding angles of $\mathcal{T}$. Thus $\limsup_n \Phi(P_n) \leq \Phi(P)$.

Conversely, suppose $\phi = \liminf_n \Phi(P_n)$. Fix $\epsilon > 0$ and suppose $\mathcal{T}_n$ is a $(\phi + \epsilon)$-triangulation of P_n. Passing to a subsequence, if necessary, we assume $\phi = \lim_n \Phi(P_n)$ and $\Phi(P_n) < \phi + \epsilon$ for all n. As in the proof of Lemma 5.1, we may construct a

quasiconformal map f_n from the interior of P_n to the interior of P with dilatation tending uniformly to zero as $n \nearrow \infty$. By Lemma 4.1, the push-forward of $\mathcal{T}_n$ under f_n is a triangulation with maximum angle $\leq \phi + 2\epsilon$ if n is large enough (it may also be necessary to choose $\mathcal{T}_n$ sufficiently fine). Thus P has $(\phi + 2\epsilon)$-triangulations for every $\epsilon > 0$, so $\Phi(P) \leq \liminf_n \Phi(P_n)$. Thus Φ is continuous at P.

If $\phi > 60$, then $\mathcal{E}(N, \phi) = \{P \in \mathcal{P}_N : \Phi(P) \leq \phi\}$ is the same as the set of N-gons that have a ϕ-triangulations (for $\phi = 60^\circ$ the latter is a subset of the former), so it is a closed set. Similarly for $\mathcal{F}(N, \phi) = \{P \in \mathcal{P}_N : \Phi(P) = \phi\}$. Corollary 1.10 shows that the $\mathcal{F}(N, 72^\circ)$ contains every polygon with all angles $\geq 144^\circ$; this is an open set for $N \geq 10$. Our remark following the proof of Corollary 1.8 shows that every axis-parallel polygon is also in the interior of $\mathcal{F}(N, 72^\circ)$ for $N \geq 4$.

To see that $\mathcal{F}(N, \frac{5}{7}90^\circ)$ has interior for N large enough, consider the polygon P in Figure 28. Note P has eight 60°-vertices, one 300° vertex and a large number of $180^\circ + \epsilon$ vertices, where ϵ may be as small as we wish. For $\phi \leq \frac{5}{7} \cdot 90^\circ$, the only ϕ-admissible labels for the 60°, 180° and 300° vertices are 1, 3 and 5 respectively (see Figure 8). Thus in this range $\kappa(\phi) = 6 - 8(3-1) - 1(3-5) = 6 - 16 + 2 = -8 < 0$. Therefore, we must be in Case 2 of Theorem 1.1 and $\phi = \frac{5}{7} \cdot 90^\circ$ is the sharp bound. Any small perturbation of P has the same vertex labels, so P is in the interior of $\mathcal{F}(N, 72^\circ)$.

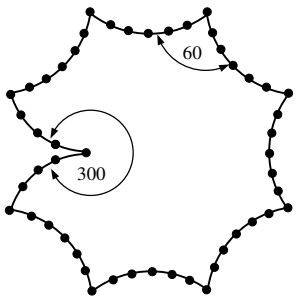

FIGURE 28. This polygon has optimal angle bound $\phi = \frac{5}{7} \cdot 90^\circ$, and so does every small perturbation, showing the set of such polygons has non-empty interior.

Finally, for any angle $\phi \in (60^\circ, 90^\circ] \setminus \{\frac{5}{7} \cdot 90^\circ, 72^\circ\}$, having sharp bound ϕ means that one or more of the angles of ϕ lies on the boundary of a shaded triangle in Figure 8 (otherwise we could decrease ϕ slightly and still meet the criteria of Theorem 1.1).

This means three adjacent points on P form an angle from a certain finite set of possibilities depending only on ϕ. Therefore $\mathcal{F}(N, \phi)$ has co-dimension at least 1. □

15. Minmax versus Maxmin

We recall some notation from Section 1. For $0 < \phi < 60°$ we define $\widetilde{I}(\phi) = [\phi, 180° - 2\phi]$; any triangle having smallest angle ϕ has all its angles inside $\widetilde{I}(\phi)$. Define a labeling L to be ϕ-lower-admissible if $\theta_v \in L(v) \cdot \widetilde{I}(\phi)$ where θ_v is the angle of P at $v \in V_P$. See Figure 29. The curvature $\kappa(L)$ the same as before, and $\widetilde{\mathcal{K}}(\phi)$ is the set of curvatures of ϕ-lower-admissible labelings. We set $\widetilde{\kappa}(\phi)$ to be the element of this set closest to 0 (equal to ∞ if no lower-admissible labeling exists). A ϕ-lower-triangulation means a triangulation will all angles $\geq \phi$.

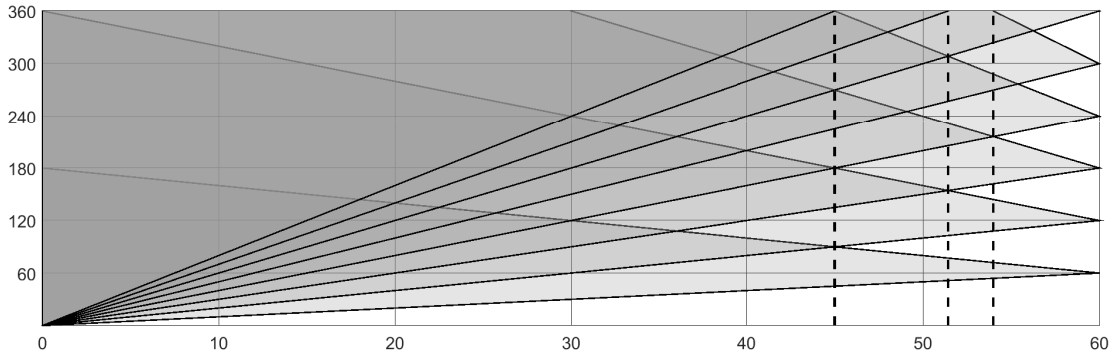

Figure 29. P has an ϕ-lower-admissible labeling if and only if all its angles lie in the intersection of the union of shaded triangles with the vertical line above ϕ. For $\phi \leq 45°$, this only depends on the size of the smallest angle. The dashed lines indicate $\phi = 45°$ and the two transition angles in Theorem 1.12.

Proof of Theorem 1.12. First consider necessity of the stated conditions. By definition, having a ϕ-lower-triangulation means that a lower-admissible labeling exists; this is Case 1. If every angle of the triangulation is greater than 45°, then every angle is also strictly less than 90°. This implies every vertex in $\partial\mathcal{T} \setminus V_P$ has degree 3, so (1.1) becomes

$$\sum_{v \in \text{int}(\mathcal{T})} \kappa(v) + \sum_{v \in V_P} \kappa(v) = 6. \tag{15.1}$$

If we also have $\phi > \frac{1}{7} \cdot 360^\circ$, then there are no interior vertices of degree seven, so the first term in (15.1) is non-negative. Thus $\kappa(L) = 6 - \sum_{v \in V_P} \kappa(v) \geq 0$, as desired. If $\phi > 54^\circ$, then every $v \in \text{int}(\mathcal{T})$ has degree six, so $\kappa(L) = 0$ as desired.

To prove sufficiency, we simply follow the proof of Theorem 1.1, except that in this case the 420°-trick is the first one eliminated at $\phi = \frac{1}{7} \cdot 360^\circ \approx 51.4286$, and the 120°-trick is eliminated at $\phi = 54^\circ$. □

Proof of Corollary 1.13 . The linear time calculation of $\widetilde{\Phi}(P)$ is very similar to the calculation of $\Phi(P)$ described earlier, so we only note a few changes to the proof of Corollary 1.6. We define

$$\widetilde{\phi}_\infty = \sup\{\phi \in [60^\circ, 90^\circ] : \widetilde{\kappa}(\phi) < \infty\}$$

$$\widetilde{\phi}_0 = \sup\{\phi \in [60^\circ, 90^\circ] : \widetilde{\kappa}(\phi) = 0\}.$$

Since $\widetilde{I}(0) = [0^\circ, 180^\circ]$ it is easy to check that $\widetilde{\kappa}(0^\circ) = 0$, so $0 < \widetilde{\phi}_0 \leq \widetilde{\phi}_\infty$. If $\widetilde{\kappa}(\widetilde{\phi}_\infty) = 0$, then $\widetilde{\phi}_0 = \widetilde{\phi}_\infty$, and this common value equals $\widetilde{\Phi}(P)$. If $\widetilde{\kappa}(\widetilde{\phi}_\infty) > 0$, Then $\widetilde{\kappa}(\phi)$ is increasing and non-negative and

- if $\widetilde{\phi}_\infty \leq 54^\circ$, then $\widetilde{\Phi}(P) = \widetilde{\phi}_\infty$;
- if $\widetilde{\phi}_\infty > 54^\circ$, then $\widetilde{\Phi}(P) = 54^\circ$.

Otherwise, $\widetilde{\kappa}(\widetilde{\phi}_\infty) < 0$, and $\widetilde{\kappa}(\phi)$ is decreasing and non-positive and

- if $\widetilde{\phi}_\infty \leq \frac{4}{7} \cdot 90^\circ$, then $\widetilde{\Phi}(P) = \widetilde{\phi}_\infty$;
- if $\widetilde{\phi}_\infty > \frac{4}{7} \cdot 90^\circ$, then $\widetilde{\Phi}(P) = \widetilde{\phi}_0$.

Thus we are reduced to calculating $\widetilde{\phi}_0$ and $\widetilde{\phi}_\infty$. Each of these can be done in linear time, just as in the proof Corollary 1.6 (the logic is the same, although the formulas are slightly different since $I(\phi)$ is different from $\widetilde{I}(\phi)$). □

Proof of Corollary 1.14. If $\phi > 45^\circ$, then every triangulation angle is $\leq 180^\circ - 2\phi < 90^\circ$, so we are done. For $\phi \leq 45^\circ$, the angles created in the proof is always acute, except possible near a vertex v of P. If v has angle θ_v we choose the largest possible ϕ-lower-admissible label $L(v)$ for v. This means $L(v) \cdot \phi \leq \theta_v < (1 + L(v)) \cdot \phi$, so

$$\phi \leq \theta_v / L(v) < (1 + 1/L(v)) \cdot \phi \leq 2 \cdot \phi \leq 90^\circ.$$

Thus angles in a neighborhood of each vertex are in the correct range, and interior vertices of degree five or seven only introduce angles $\geq \frac{4}{7} \cdot 90^\circ > \phi$ and $\leq 72^\circ$. □

Proof of Corollary 1.15 . See Figure 29. Note that if $\phi \leq 45°$, then $\bigcup_k k \cdot \widetilde{I}(\phi) = [\phi, \infty)$, so P has a ϕ-lower-admissible labeling if and only if $\theta_{\min} \geq \phi$. □

16. Questions and remarks

We observed in the introduction that the number of elements of an angle-optimal triangulation of an N-gon will not satisfy a polynomial bound in N in general.

Question 16.1. *Can we find a ϕ-triangulation with the minimal number of elements, say in time comparable to the number of elements output?*

Question 16.2. *Can we estimate, to within a bounded factor, the smallest number of triangles needed in terms of the geometry of P?*

Question 16.3. *Is computing the minimal number of triangles required by an angle-optimal triangulation NP hard?*

Our proof of Theorem 1.1 does not give anything near the optimal number of triangles. Each edge e of the polygon P has a harmonic measure $\omega(z, e)$ that depends on a choice of base point z in the interior of P. This is the point that is mapped to the origin by our conformal map to the disk, and $\omega(z, e)$ is the length of the image of e on the unit circle (usually normalized so the circle has length 1). Our construction will generally then use $O(\inf_z \inf_e \omega(e)^{-2})$ triangles. In the case of a $1 \times r$ rectangle, $\omega(z, e) \simeq \exp(-\pi r/2)$ for at least one of the short ends e, no matter how we choose the base point z, so our proof gives an exponential number of triangles as a function of r. However, it is easy to see by a direct construction that only $O(r)$ triangles are needed to achieve the optimal angle bound 72°. See Figure 30. Here we have chosen a P' that mimics the overall shape of the rectangle, and obtain $O(r)$ triangles, at the cost of introducing many more degree five vertices into the triangulation when we apply the 120°-trick.

Question 16.4. *Does choosing a $60°$-polygon P' to "mimic" P in some precise sense always give a nearly optimal number of triangles, at least if the optimal angle bound ϕ is $\geq 72°$?*

Recall that a planar straight line graph (PSLG) is a disjoint collection of open line segments, together with a finite set of points, including all the endpoints of all

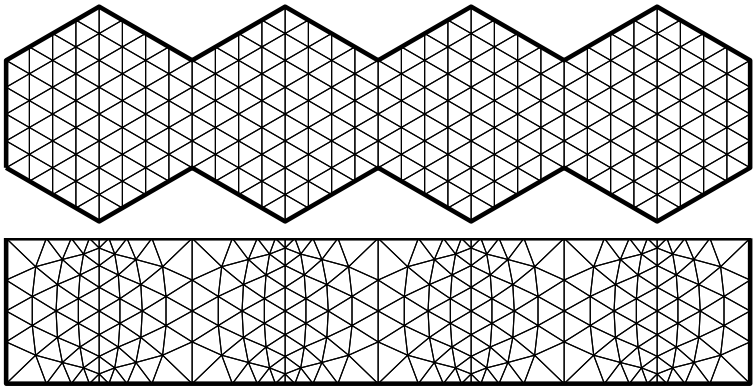

FIGURE 30. A different choice of P' leads to a number of triangles that is within a bounded factor of optimal. In this figure we have to make the grid finer and apply the 120°-trick to get rid of certain boundary vertices with angle 90°.

the segments. Triangulating a PSLG usually means to triangulate its convex hull so that the triangulation "conforms" to the PSLG, i.e., the edges of the PSLG are covered by edges of the triangulation and every vertex of the PSLG is a vertex of the triangulation. Simple polygons are a special case of a PSLG where the edges are joined end-to-end, but triangulating PSLGs tends to be more difficult, since triangles must "match up" across any edges of the PSLG that are not on the convex hull boundary.

Question 16.5. *Does every PSLG with N vertices have an acute conforming triangulation with $O(N^2)$ elements?*

It is known that some examples require $\simeq N^2$ triangles, and that $O(N^{5/2})$ triangles always suffice. See [16]. For polygons, $O(N)$ triangles always suffice, e.g., [9] gives a non-obtuse triangulation of this size, and [46] or [61] convert it to an acute triangulation of comparable size.

Question 16.6. *Does every PSLG with minimal interior angle* 36° *have a* 72° *conforming triangulation?*

Question 16.7. *If a PSLG has minimum angle θ, does it have conforming triangulation with all angles in the interval $J(\theta) = [\theta, 90° - \min(\theta, 36°)/2]$?*

One of the surprising results of this paper is that angle optimal triangulations always exist, except for 60°-polygons with two edges having irrational length ratio. The corresponding question for length-optimal triangulations is open.

Question 16.8. *Does a polygon in general position have a minimal weight Steiner triangulation (MWST), i.e, a triangulation that minimizes the total edge length ?*

Such a triangulation need not exist if we allow three co-linear vertices, [15]. An algorithm for approximating the infimum to within a constant factor is given in David Eppstein's paper [30]. If there are not always minimal weight triangulations, how do the triangulations approaching the minimum behave?

Question 16.9. *Are there simple N-gons where approximating the minimal weight triangulation requires the number of triangles to tend to ∞? If not, prove a bound on the number of triangles needed.*

Without Steiner points, a minimum weight triangulation (MWT) for a simple N-gon obviously exists (there are only finitely many possible triangulations), and can be computed in time $O(N^3)$ by [34], [40]. For point sets, computing the minimum is NP-hard [49]. How difficult are these problems with Steiner points?

One of the referees of an earlier draft of this paper pointed out several similarities between it and [57] by William Thurston, such as using vertex degrees to define the curvature of a combinatorial triangulation, and the special role played by equilateral grid polygons. Thurston's paper deals with characterizing combinatorial triangulations of the 2-sphere that have non-negative curvature (i.e., every vertex has degree at most six), by interpreting them as lattice points in a higher dimensional complex hyperbolic space defined using cone metrics on the sphere. The current paper constructs specific planar embeddings of triangulations whose curvature properties are forced by the desired geometry, e.g., Corollary 1.17 says precisely how many vertices of degree other than six are needed in an angle optimal triangulation. If we glue two copies of the polygon along the boundaries, we get a triangulation of the sphere with specified curvatures. When these are all positive, can the results in [57] help construct an optimal triangulation faster? Can they help find an optimal triangulation with fewest elements (or nearly fewest)? Do Thurston's ideas extend to cover the case when negative curvature vertices are needed?

Corollary 1.11 showed the that set of N-gons with $\Phi(P) = 72°$ contains an open set, and thus it should have positive measure with respect to any measure on the space of N-gons that is absolutely continuous with respect to volume measure on $\mathbb{R}^{2N}$. What are natural examples of such measures, i.e., what is a random polygon? Figure 31 show the result of computing the optimal upper bound for a billion random 10-tuples summing to $1440 = 8 \cdot 180$. This is meant to simulate a random 10-gon, but the lists were generated by choosing ten random numbers in $[0, 1]$ and renormalizing to get the correct sum. This will sometimes generate angles $> 360°$ and since side lengths are not accounted for, the lists don't correctly represent the angles of simple polygons. However, the predicted mass at $72°$ is clearly visible (about 20% of the total mass), but no peak appears at $\frac{5}{7} \cdot 90°$. Is $N = 10$ too small for this open set to occur in Corollary 1.11? If so, what is the smallest N for which it does occur?

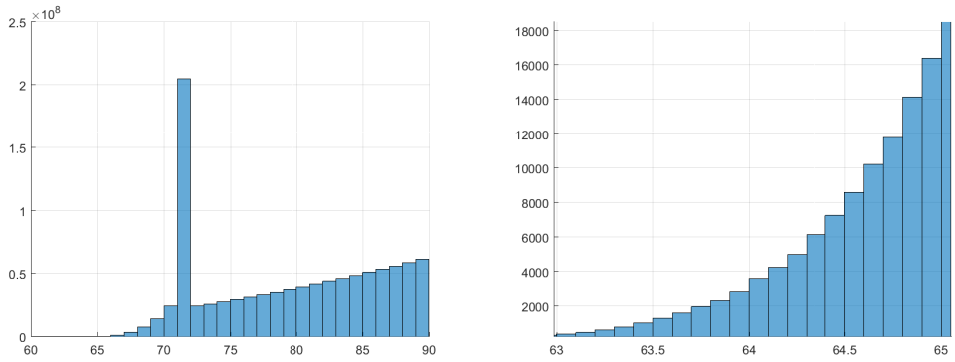

FIGURE 31. The distribution of optimal upper bounds over 10^9 random samples as described in the text. On the left is a histogram based on $1°$ bins. The spike a $72°$ is evident. On the right is an enlargement near $64°$ using $.1°$ bins. No spike at $\frac{5}{7} \cdot 90° \approx 64.26°$ is visible.

REFERENCES

[1] L. V. Ahlfors. *Lectures on quasiconformal mappings*. The Wadsworth & Brooks/Cole Mathematics Series. Wadsworth & Brooks/Cole Advanced Books & Software, Monterey, CA, 1987. With the assistance of Clifford J. Earle, Jr., Reprint of the 1966 original.

[2] A. Alexandrescu. Fast deterministic selection. In *16th Symposium on Experimental Algorithms*, volume 75 of *LIPIcs. Leibniz Int. Proc. Inform.*, pages Art. 24, 19. Schloss Dagstuhl. Leibniz-Zent. Inform., Wadern, 2017.

[3] B. Aronov, T. Asano, and S. Funke. Optimal triangulation with Steiner points. In *Algorithms and computation*, volume 4835 of *Lecture Notes in Comput. Sci.*, pages 681–691. Springer, Berlin, 2007.

[4] B. Aronov, T. Asano, and S. Funke. Optimal triangulations of points and segments with Steiner points. *Internat. J. Comput. Geom. Appl.*, 20(1):89–104, 2010.
[5] B.S. Baker, E. Grosse, and C.S. Rafferty. Nonobtuse triangulation of polygons. *Discrete Comput. Geom.*, 3(2):147–168, 1988.
[6] M. Bern. Adaptive mesh generation. In *Error estimation and adaptive discretization methods in computational fluid dynamics*, volume 25 of *Lect. Notes Comput. Sci. Eng.*, pages 1–46. Springer, Berlin, 2003.
[7] M. Bern, H. Edelsbrunner, D. Eppstein, S. Mitchell, and T. S. Tan. Edge insertion for optimal triangulations. In *LATIN '92 (São Paulo, 1992)*, volume 583 of *Lecture Notes in Comput. Sci.*, pages 46–60. Springer, Berlin, 1992.
[8] M. Bern, D. Eppstein, and J. Gilbert. Provably good mesh generation. *J. Comput. System Sci.*, 48(3):384–409, 1994. 31st Annual Symposium on Foundations of Computer Science (FOCS) (St. Louis, MO, 1990).
[9] M. Bern, S. Mitchell, and J. Ruppert. Linear-size nonobtuse triangulation of polygons. *Discrete Comput. Geom.*, 14(4):411–428, 1995. ACM Symposium on Computational Geometry (Stony Brook, NY, 1994).
[10] M. Bern and P. Plassmann. Mesh generation. In *Handbook of computational geometry*, pages 291–332. North-Holland, Amsterdam, 2000.
[11] M. Bern, J.R. Shewchuk, and N. Amenta. Triangulations and mesh generation. In J.E. Goodman, J. O'Rourke, and C.D. Tóth, editors, *Handbook of discrete and computational geometry, Third edition*, chapter 29, pages 266–290. CRC Press, Boca Raton, FL, 2017.
[12] C. J. Bishop. Conformal welding and Koebe's theorem. *Ann. of Math. (2)*, 166(3):613–656, 2007.
[13] C.J. Bishop. Uniformly acute triangulations for polygons. to appear in *Discrete Comput. Geom.*
[14] C.J. Bishop. Uniformly acute triangulations for PSLGs. to appear in *Discrete Comput. Geom.*
[15] C.J. Bishop. Minimal weight Steiner triangulation need not exist. 2007. preprint.
[16] C.J. Bishop. Nonobtuse triangulations of PSLGs. *Discrete Comput. Geom.*, 56(1):43–92, 2016.
[17] C.J. Bishop. Optimal angle bounds for Steiner triangulations of polygons. In *Proceedings of the 2022 Annual ACM-SIAM Symposium on Discrete Algorithms (SODA)*, pages 3127–3143. [Society for Industrial and Applied Mathematics (SIAM)], Philadelphia, PA, 2022.
[18] M. Blum, V. Pratt, R.E. Tarjan, R.W. Floyd, and R.L. Rivest. Time bounds for selection. *J. Comput. System Sci.*, 7:448–461, 1973.
[19] Yu. D. Burago and V. A. Zalgaller. Polyhedral embedding of a net. *Vestnik Leningrad. Univ.*, 15(7):66–80, 1960.
[20] B. Chazelle and D.P. Dobkin. Optimal convex decompositions. In *Computational geometry*, volume 2 of *Mach. Intelligence Pattern Recogn.*, pages 63–133. North-Holland, Amsterdam, 1985.
[21] L. Paul Chew. Guaranteed-quality mesh generation for curved surfaces. In *Proceedings of the Ninth Annual Symposium on Computational Geometry*, SCG '93, page 274–280, New York, NY, USA, 1993. Association for Computing Machinery.
[22] E.B. Christoffel. Sul problema della tempurature stazonaire e la rappresetazione di una data superficie. *Ann. Mat. Pura Appl. Serie II*, pages 89–103, 1867.
[23] H.T. Croft, K.J. Falconer, and R.K. Guy. *Unsolved problems in geometry*. Problem Books in Mathematics. Springer-Verlag, New York, 1991.
[24] T.A Driscoll. Algorithm 843: Improvements to the Schwarz-Christoffel Toolbox for MATLAB. *ACM Transactions on Mathematical Software (TOMS)*, 31(2):239–251, 2005.

[25] T.A. Driscoll and L.N. Trefethen. *Schwarz-Christoffel mapping*, volume 8 of *Cambridge Monographs on Applied and Computational Mathematics*. Cambridge University Press, Cambridge, 2002.
[26] H. Edelsbrunner. Triangulations and meshes in computational geometry. In *Acta Numerica, 2000*, volume 9 of *Acta Numer.*, pages 133–213. Cambridge Univ. Press, Cambridge, 2000.
[27] H. Edelsbrunner. *Geometry and topology for mesh generation*, volume 7 of *Cambridge Monographs on Applied and Computational Mathematics*. Cambridge University Press, Cambridge, 2006. Reprint of the 2001 original.
[28] H. Edelsbrunner, T.S. Tan, and R. Waupotitsch. An $O(n^2 \log n)$ time algorithm for the minmax angle triangulation. *SIAM J. Sci. Statist. Comput.*, 13(4):994–1008, 1992.
[29] D. Eppstein. Acute square triangulation. Webpage https://www.ics.uci.edu/ eppstein/junkyard/acute-square/, Accessed: January 2, 2021.
[30] D. Eppstein. Approximating the minimum weight triangulation. In *Proceedings of the Third Annual ACM-SIAM Symposium on Discrete Algorithms (Orlando, FL, 1992)*, pages 48–57. ACM, New York, 1992.
[31] H. Erten and A. Üngör. Computing acute and non-obtuse triangulations. In *CCCG 2007, Ottawa, Cananda*. 2007.
[32] J.B. Garnett and D.E. Marshall. *Harmonic measure*, volume 2 of *New Mathematical Monographs*. Cambridge University Press, Cambridge, 2005.
[33] J. L. Gerver. The dissection of a polygon into nearly equilateral triangles. *Geom. Dedicata*, 16(1):93–106, 1984.
[34] P. D. Gilbert. New results in planar triangulations. Technical report, Tech. Rep. R-850, Univ. Illinois Coordinated Science Lab., 1979.
[35] J.E. Goodman, J. O'Rourke, and C.D. Tóth, editors. *Handbook of discrete and computational geometry*. Discrete Mathematics and its Applications (Boca Raton). CRC Press, Boca Raton, FL, 2018. Third edition of [MR1730156].
[36] D. H. Hamilton. Conformal welding. In *Handbook of complex analysis: geometric function theory, Vol. 1*, pages 137–146. North-Holland, Amsterdam, 2002.
[37] J. Itoh and T. Zamfirescu. Acute triangulations of the regular icosahedral surface. *Discrete Comput. Geom.*, 31(2):197–206, 2004.
[38] M. Keil and J. Snoeyink. On the time bound for convex decomposition of simple polygons. *Internat. J. Comput. Geom. Appl.*, 12(3):181–192, 2002.
[39] R. Kenyon. Tilings of convex polygons. *Ann. Inst. Fourier (Grenoble)*, 47(3):929–944, 1997.
[40] G. T. Klincsek. Minimal triangulations of polygonal domains. *Ann. Discrete Math.*, 9:121–123, 1980.
[41] S. Korotov and J. Stańdo. Nonstandard nonobtuse refinements of planar triangulations. In *Conjugate gradient algorithms and finite element methods*, Sci. Comput., pages 149–160. Springer, Berlin, 2004.
[42] C.L. Lawson. *Software for C^1 surface interpolation*, pages ix+388. Academic Press [Harcourt Brace Jovanovich Publishers], New York, 1977. Publication of the Mathematics Research Center, No. 39.
[43] D. T. Lee and A. K. Lin. Generalized Delaunay triangulation for planar graphs. *Discrete Comput. Geom.*, 1(3):201–217, 1986.
[44] O. Lehto and K. I. Virtanen. *Quasiconformal mappings in the plane*. Springer-Verlag, New York-Heidelberg, second edition, 1973. Translated from the German by K. W. Lucas, Die Grundlehren der mathematischen Wissenschaften, Band 126.

[45] J. Y. S. Li and H. Zhang. Nonobtuse remeshing and mesh decimation. In *SGP '06: Proceedings of the fourth Eurographics symposium on Geometry processing*, pages 235–238, Aire-la-Ville, Switzerland, Switzerland, 2006. Eurographics Association.
[46] H. Maehara. Acute triangulations of polygons. *European J. Combin.*, 23(1):45–55, 2002.
[47] E.A. Melissaratos and D.L. Souvaine. Coping with inconsistencies: a new approach to produce quality triangulations of polygonal domains with holes. In *SCG '92: Proceedings of the eighth annual symposium on computational geometry*, pages 202–211, New York, NY, USA, 1992. ACM.
[48] S.A. Mitchell. Approximating the maxmin-angle covering triangulation. volume 7, pages 93–111. 1997. Fifth Canadian Conference on Computational Geometry (Waterloo, ON, 1993).
[49] W. Mulzer and G. Rote. Minimum-weight triangulation is NP-hard. *J. ACM*, 55(2):Art. 11, 29, 2008.
[50] Z. Nehari. *Conformal mapping*. Dover Publications Inc., New York, 1975. Reprinting of the 1952 edition.
[51] S. Rohde. On conformal welding and quasicircles. *Michigan Math. J.*, 38:111–116, 1991.
[52] J. Ruppert. A new and simple algorithm for quality 2-dimensional mesh generation. In *Proceedings of the Fourth Annual ACM-SIAM Symposium on Discrete Algorithms (Austin, TX, 1993)*, pages 83–92, New York, 1993. ACM.
[53] S. Saraf. Acute and nonobtuse triangulations of polyhedral surfaces. *European J. Combin.*, 30(4):833–840, 2009.
[54] H.A. Schwarz. Confome abbildung der oberfläche eines tetraeders auf die oberfläche einer kugel. *J. Reine Ange. Math.*, pages 121–136, 1869. Also in collected works, [55], pp. 84-101.
[55] H.A. Schwarz. *Gesammelte Mathematische Abhandlungen*. Springer, Berlin, 1890.
[56] J. R. Shewchuk. Delaunay refinement algorithms for triangular mesh generation. *Comput. Geom.*, 22(1-3):21–74, 2002. 16th ACM Symposium on Computational Geometry (Hong Kong, 2000).
[57] William P. Thurston. Shapes of polyhedra and triangulations of the sphere. In *The Epstein birthday schrift*, volume 1 of *Geom. Topol. Monogr.*, pages 511–549. Geom. Topol. Publ., Coventry, 1998.
[58] L. N. Trefethen and T.A. Driscoll. Schwarz-Christoffel mapping in the computer era. In *Proceedings of the International Congress of Mathematicians, Vol. III (Berlin, 1998)*, number Extra Vol. III, pages 533–542 (electronic), 1998.
[59] L.N. Trefethen. Numerical computation of the Schwarz-Christoffel transformation. *SIAM J. Sci. Statist. Comput.*, 1(1):82–102, 1980.
[60] W. T. Tutte. The dissection of equilateral triangles into equilateral triangles. *Proc. Cambridge Philos. Soc.*, 44:463–482, 1948.
[61] L. Yuan. Acute triangulations of polygons. *Discrete Comput. Geom.*, 34(4):697–706, 2005.
[62] C.T. Zamfirescu. Survey of two-dimensional acute triangulations. *Discrete Math.*, 313(1):35–49, 2013.

C.J. Bishop, Mathematics Department, Stony Brook University, Stony Brook, NY 11794-3651

Email address: bishop@math.stonybrook.edu